P-08-103

Characterisation of micro cracks caused by core-disking

Urban Åkesson
CBI Swedish Cement and Concrete Research Institute

December 2008

Svensk Kärnbränslehantering AB
Swedish Nuclear Fuel
and Waste Management Co

Box 250, SE-101 24 Stockholm
Phone +46 8 459 84 00

ISSN 1402-3091
SKB Rapport R-08-103

Characterisation of micro cracks caused by core-disking

Urban Åkesson
CBI Swedish Cement and Concrete Research Institute

December 2008

Keywords: Core disking, Micro cracks, Image analysis.

Abstract

A quantitative study of the micro crack pattern has been carried out on thin sections from six different drill core specimens; two from Forsmark, Sweden and four from Underground Research Laboratory (URL) in Canada. The two Forsmark specimens and two of the URL specimens have been exposed to core disking. The results showed that transgranular micro cracks are mainly formed when the core disking occurs. These cracks are mostly situated within 1 mm from the large cracks that form the typical crack pattern characterizing the core disking phenomena. Between these large cracks there are very few micro cracks that can be related to core disking. There are very few transgranular cracks that not hit the mantle of the core which indicates that the transgranular cracks starts from the mantle of the core and propagate through the whole core or stop in the centre of the core.

Sammanfattning

En kvantitativ studie av mikrosprickmönstret har utförts på tunnslip tagna från sex olika borrkärneprover, två från Forsmark, Sverige och fyra från Underground Research Laboratory (URL) i Kanada. De två proverna från Forsmark och två av proverna från URL har blivit utsatta för ”core disking”. Resultaten visar att det är främst transgranulära sprickor som bildas vid core disking och dessa sprickor uppträder i huvudsak inom 1 mm från de större synliga sprickorna i proverna. Mellan dessa större sprickor har väldigt få mikrosprickor påträffats som kan härledas till core disking. Det är väldigt få transgranulära sprickor som inte träffar manteln av borrkärnan, vilket indikerar att dessa sprickor startar vid manteln och propagerar genom hela borrkärnan eller stannar i centrum av kärnan.

Contents

1	**Introduction**	7
2	**Objective and scope**	9
3	**Execution**	11
3.1	Description of the specimens	11
3.2	Testing	14
4	**Results**	15
4.1	Grain-size distribution	15
4.2	Micro crack analyses	17
	4.2.1 Part I, Linear traverse measurements	18
	4.2.2 Part II Length and Orientation of intragranular and transgranular micro cracks	30
5	**Discussion**	43

1 Introduction

This document reports the results from a quantitative study of micro cracks on six rock specimens. Two foliated granites specimens from Forsmark, Sweden and four granite and granodiorite specimens from Underground Research Laboratory (URL) in Canada.

The purpose of this project is to investigate the micro crack pattern when the rock is exposed for the core disking phenomena.

2 Objective and scope

The purpose with this project is to characterise the micro crack pattern caused by core disking. This is done using quantitative microscopy and image analysis. The different type of micro cracks is classified (intragranular = within mineral grains, transgranular = crosses several minerals and grain boundary cracks), their density parallel and perpendicular to the drill core axis. Length and orientation of transgranular and intragranular micro cracks will also be measured.

3 Execution

3.1 Description of the specimens

Figure 3-1 to 3-13 show the plan polished slabs, impregnated with epoxy containing fluorescent dye. The black rectangular shows were the thin sections were prepared.

Table 3-1. The analysed specimens. The specimens from Forsmark were foliated, therefore two specimens were prepared. A=perpendicular to the foliation and B=parallel to the foliation.

Specimen	Borehole	Length (m)	Vertical Depth (m)	Sample description
F2A	KFM01B	475.544–475.744	466.803–467.003	Ring disking
F2B	KFM01B	475.544–475.744	466.803–467.003	Ring disking
F4A	KFM01B	241.395–241.658	236.960–237.218	Ring disking
F4B	KFM01B	241.395–241.658	236.960–237.218	Ring disking
URL1A	423-009-MVP1	3.575–3.584	3.575–3.584	Solid disking
URL1B	421-012-MVP5	1.000–1.155	1.000–1.155	Solid disking
URL2	URL-5	453.890–454.100	440.410–440.610	Solid core
URL3	URL-6	13.200–13.420	13.200–13.420	Solid core

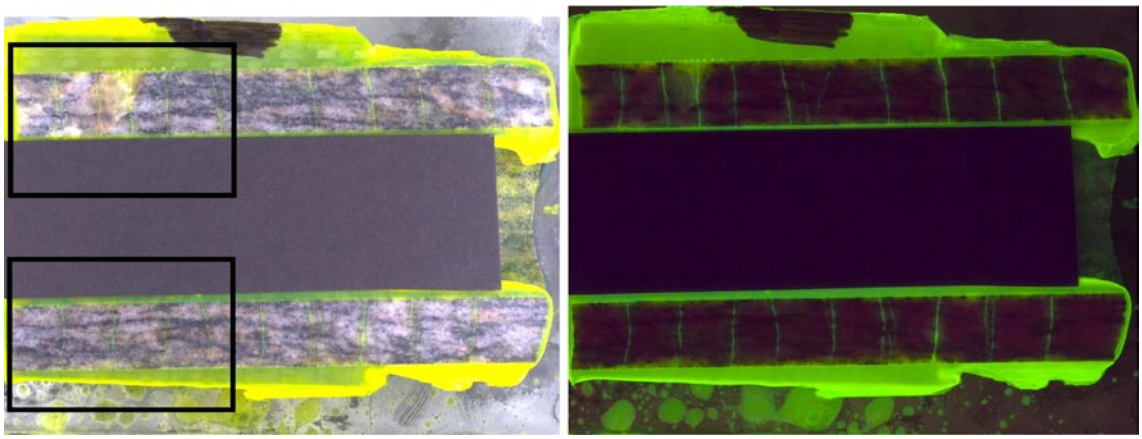

Figure 3-1 and 3-2. *Specimen F2A.*

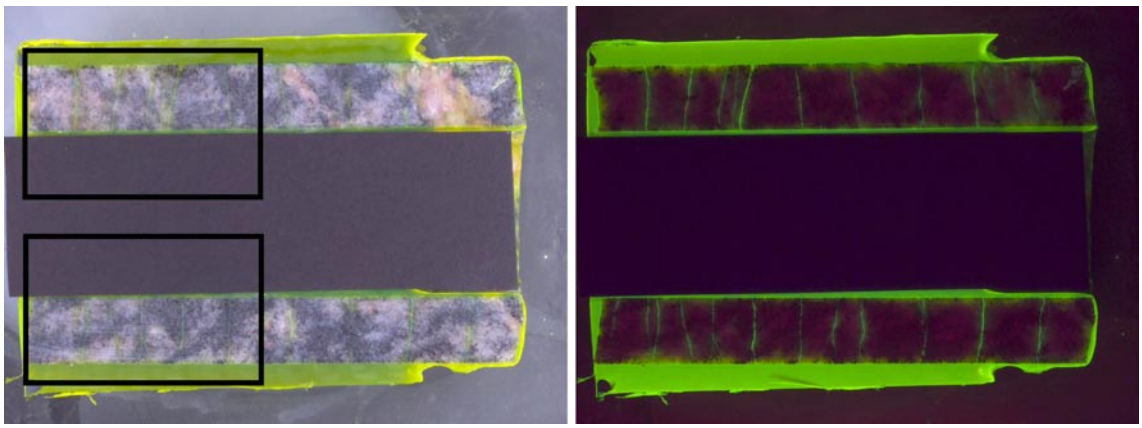

Figure 3-3 and 3-4. *Specimen F2B.*

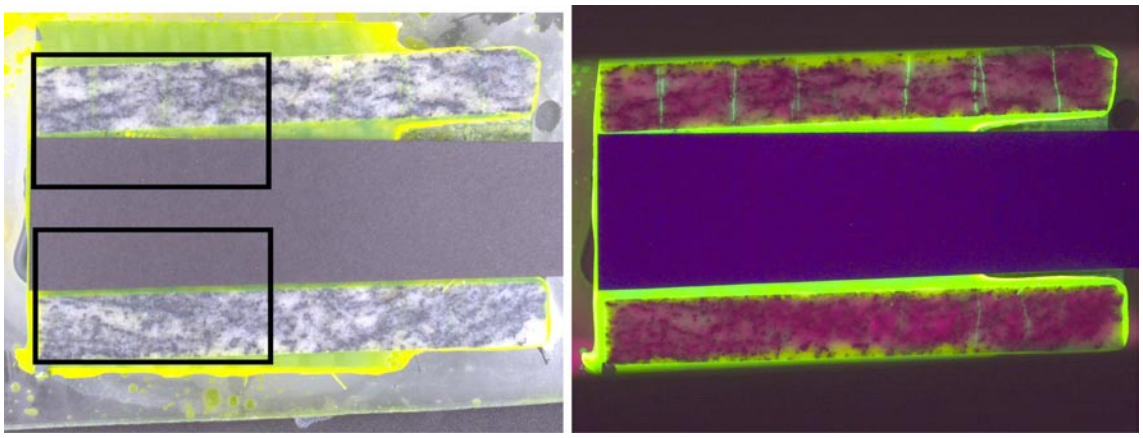

Figure 3-5 and 3-6. *Specimen F4A.*

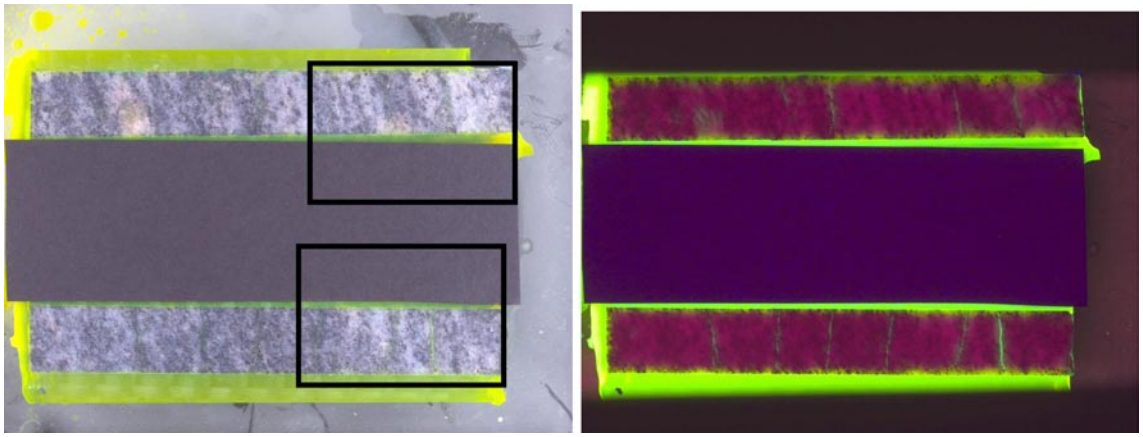

Figure 3-7 and 3-8. *Specimen F4B.*

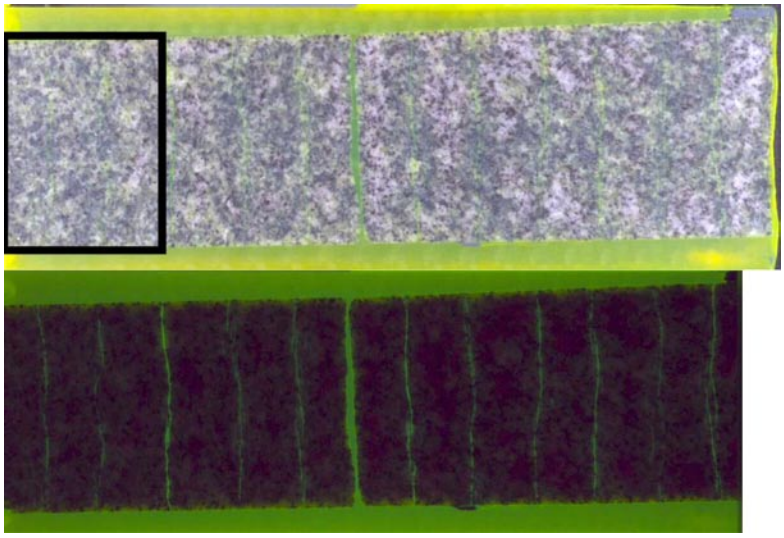

Figure 3-9 and 3-10. *Specimen URL1A.*

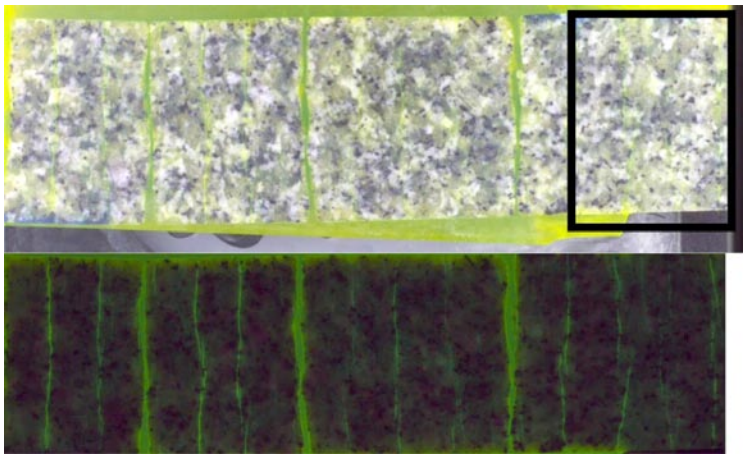

Figure 3-11 and 3-12. *Specimen URL1B.*

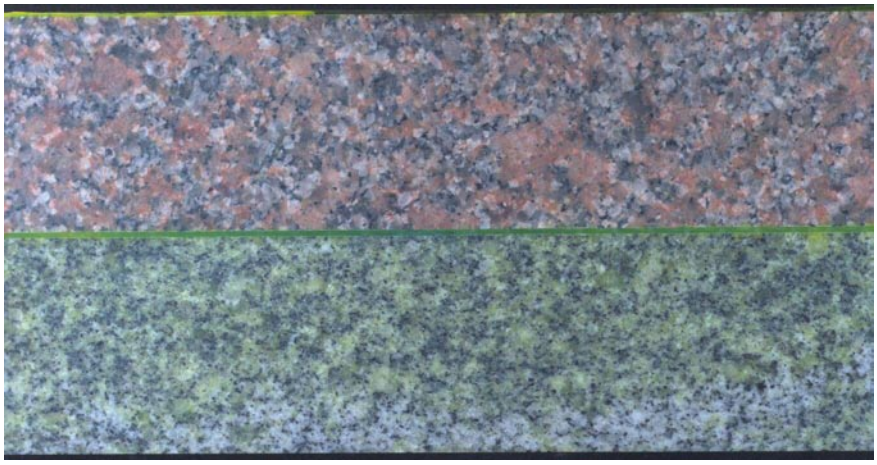

Figure 3-13. *Specimens URL2 (grey) and URL3 (red).*

3.2 Testing

Item	Activity
1	The specimens were impregnated with fluorescent epoxy.
2	The specimens were cut in half and plan polished slabs were prepared.
3	The specimens were photographed in JPEG format.
4	Thin sections were prepared, one thin section for each URL specimen and two thin sections for each Forsmark specimen.
5	The grain-size distribution was determined for each specimen using linear traverse measurements on microscopic images.
6	Micro crack characterisation. Two images taken with optical microscopy were used for the micro crack analyses, one using fluorescent light and one using polarised light. The area for each image is 2.78 x 2.10 mm per side and the image resolution is 680 x 512 pixels. The thin section was fixed on a motorised stage programmed so the images were photographed edge by edge creating a 12-image mosaic. The fluorescent and polarised images were considered together to make evaluation of where the micro cracks are formed (Figure 4-7). The density of the different crack types was determined using linear traverse measurements. The length and orientation of intragranular and transgranular cracks was determined using image analysis. The combined images were printed with a size of 272 x 269 mm and by using transparent paper, each crack-type was traced and coloured (blue = intragranular, and red = transgranular). The line-drawings were scanned into the computer, and by using RGB-thresholding technique, the length and orientation could be measured separately.

4 Results

4.1 Grain-size distribution

The grain-size distribution was determined using linear traverse measurements on microscopic images. The grain-size distribution was only determined for F2A and F4A of the Forsmark specimens.

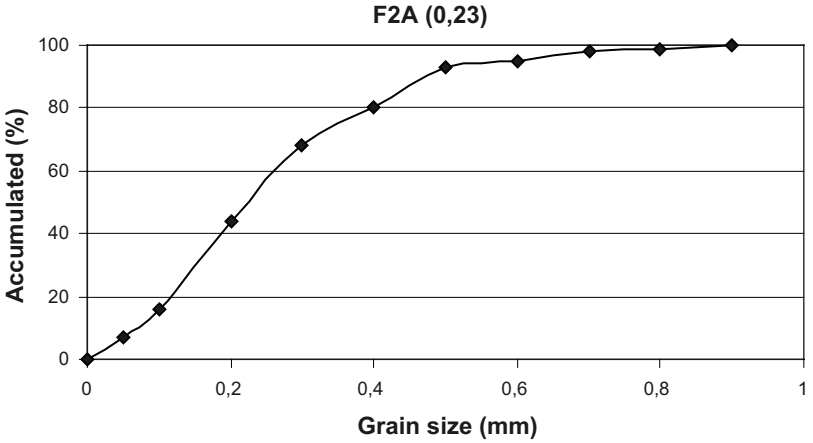

Figure 4-1. *Grain-size distribution for specimen F2A. Median value within parenthesis.*

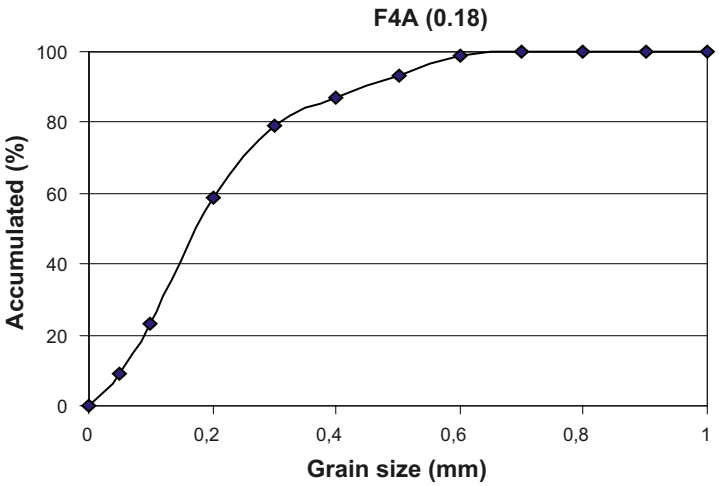

Figure 4-2. *Grain-size distribution for specimen F4A. Median value within parenthesis.*

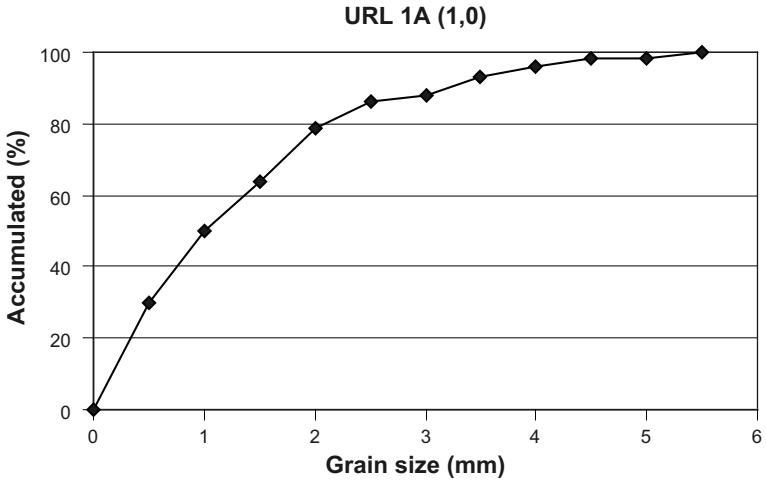

Figure 4-3. *Grain-size distribution for specimen URL1A. Median value within parenthesis.*

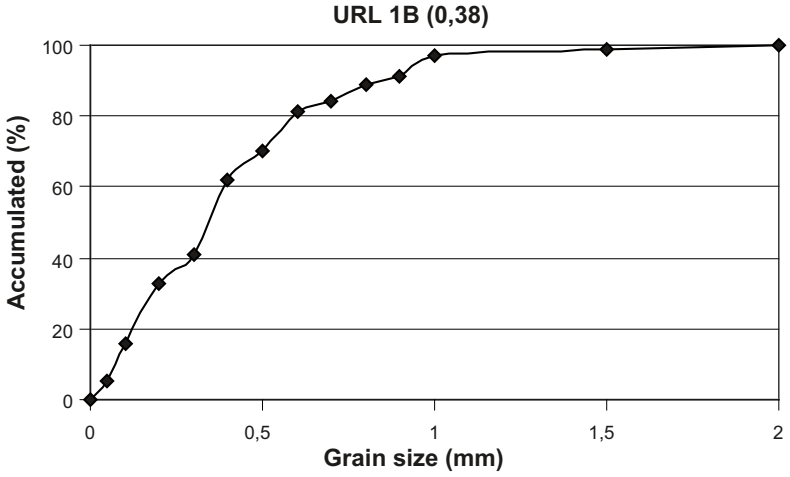

Figure 4-4. *Grain-size distribution for specimen URL1B. Median value within parenthesis.*

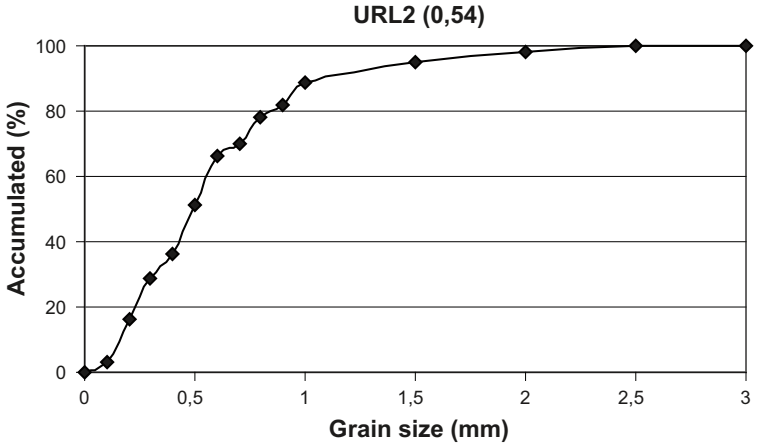

Figure 4-5. *Grain-size distribution for specimen URL2. Median value within parenthesis.*

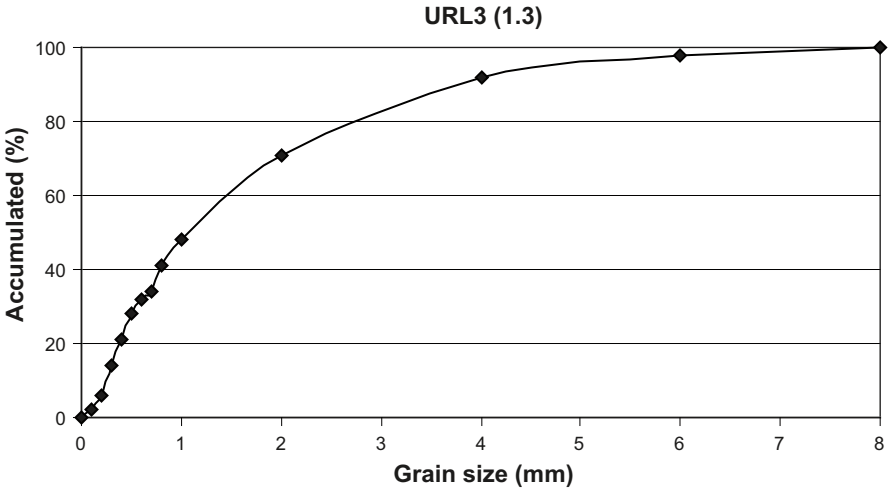

Figure 4-6. *Grain-size distribution for specimen URL3. Median value within parenthesis.*

4.2 Micro crack analyses

The micro crack analyses are divided into two parts. Part I contains the amount and distribution of different cracks expressed as amount and percentage of cracks/mm.

Part II contains measurements of length and orientation of intragranular and transgranular cracks. For the Forsmark specimens, two thin sections have been analysed (see Figures 3-1 to 3-7).

4.2.1 Part I, Linear traverse measurements

Specimen F2A1

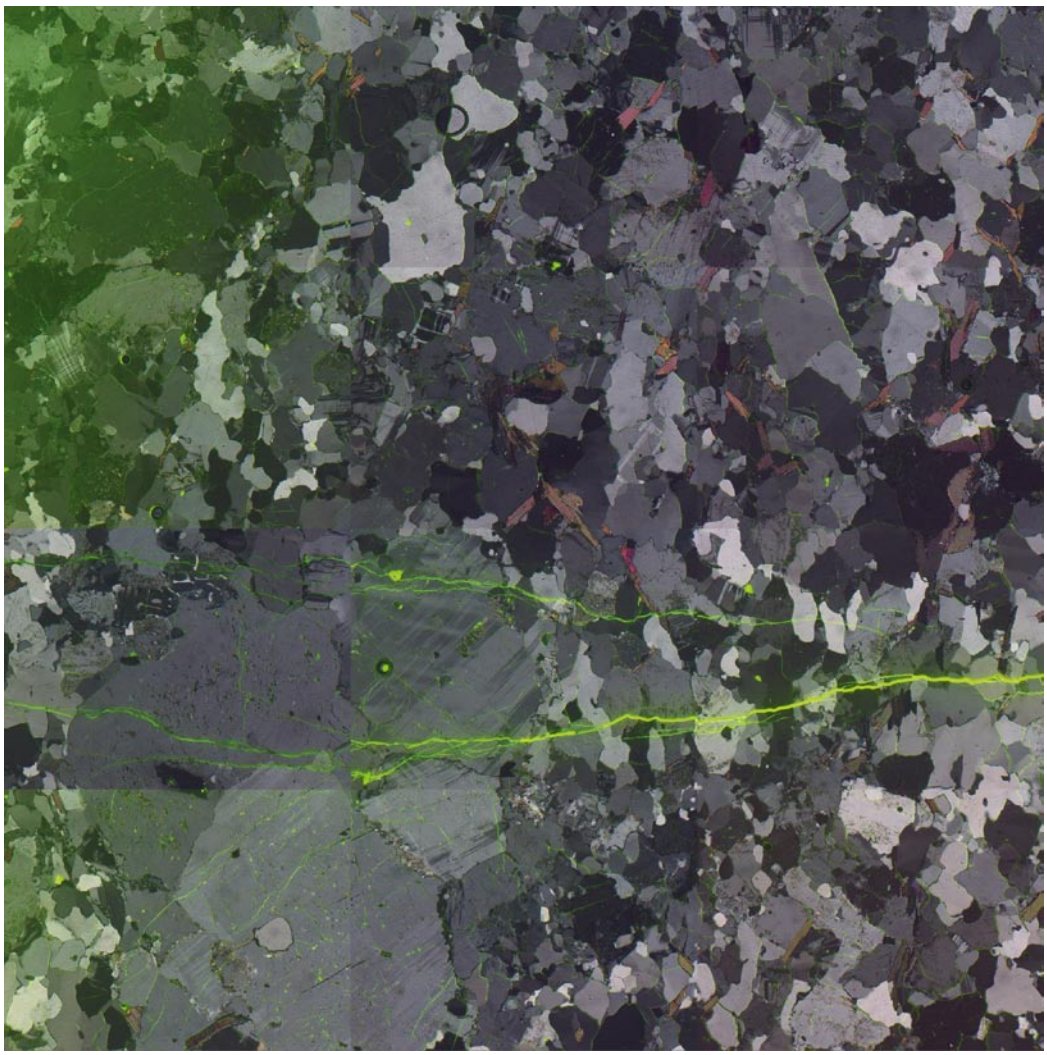

Figure 4-7. *Combined polarised and fluorescent microscopic image of specimen F2A1. Image size is 8.3 x 8.3 mm.*

Table 4-1. Crack density of specimen F2A1, based on linear traverse measurements.

Orientation	Grain boundary (cracks/mm) (%)	Intragranular (cracks/mm) (%)	Transgranular (cracks/mm) (%)	Total (cracks/mm) (%)
Parallel to drill core	2.29/86	0.34/13	0.04/1	2.67
Perpendicular to drill core	2.01/81	0.29/12	0.18/7	2.48
Ratio	1.14	1.17	0.22	1.08

Specimen F2A2

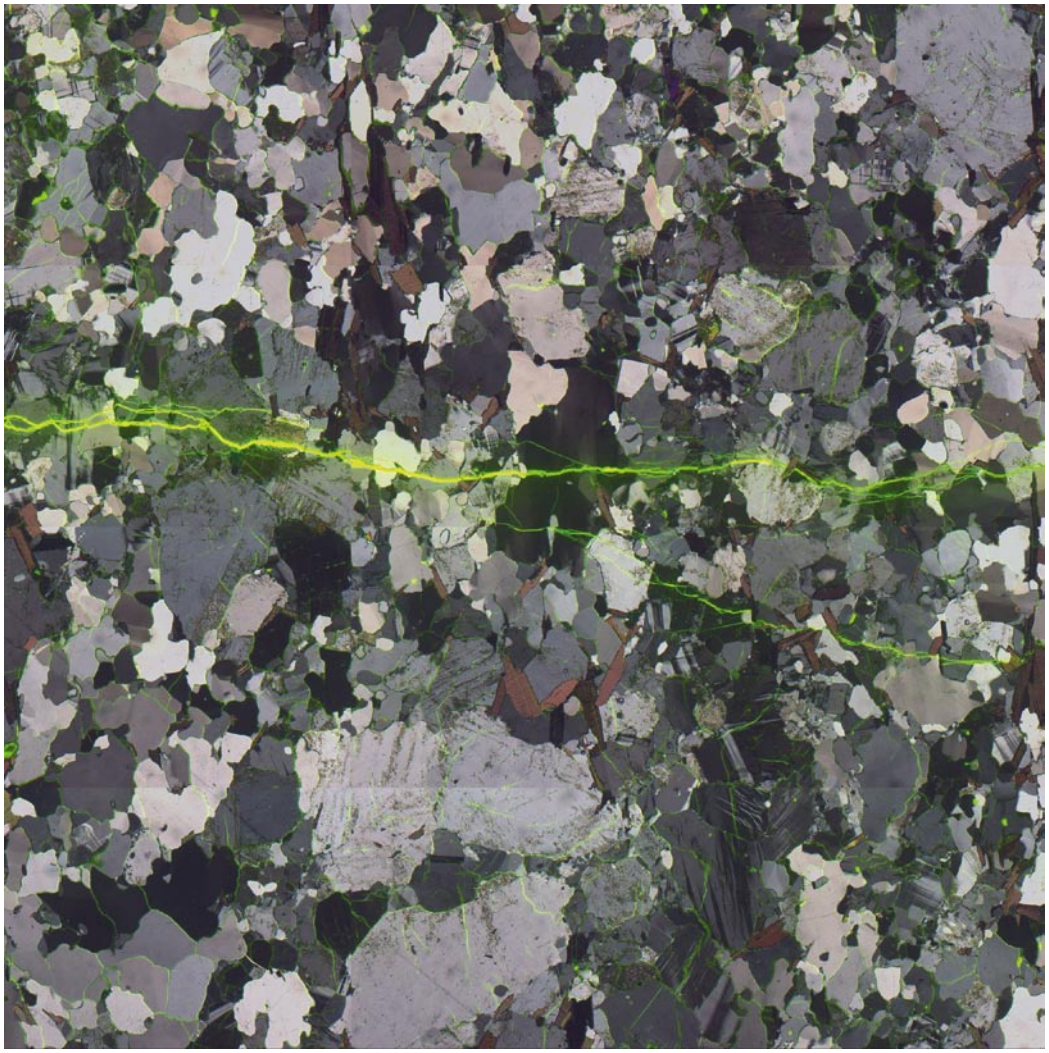

Figure 4-8. *Combined polarised and fluorescent microscopic image of specimen F2A2. Image size is 8.3 x 8.3 mm.*

Table 4-2. Crack density of specimen F2A2, based on linear traverse measurements.

Orientation	Grain boundary (cracks/mm) (%)	Intragranular (cracks/mm) (%)	Transgranular (cracks/mm) (%)	Total (cracks/mm) (%)
Parallel to drill core	3.4/86	0.49/12	0.08/2	3.97
Perpendicular to drill core	2.67/79	0.4/12	0.32/9	3.39
Ratio	1.27	1.22	0.25	1.17

Specimen F2B1

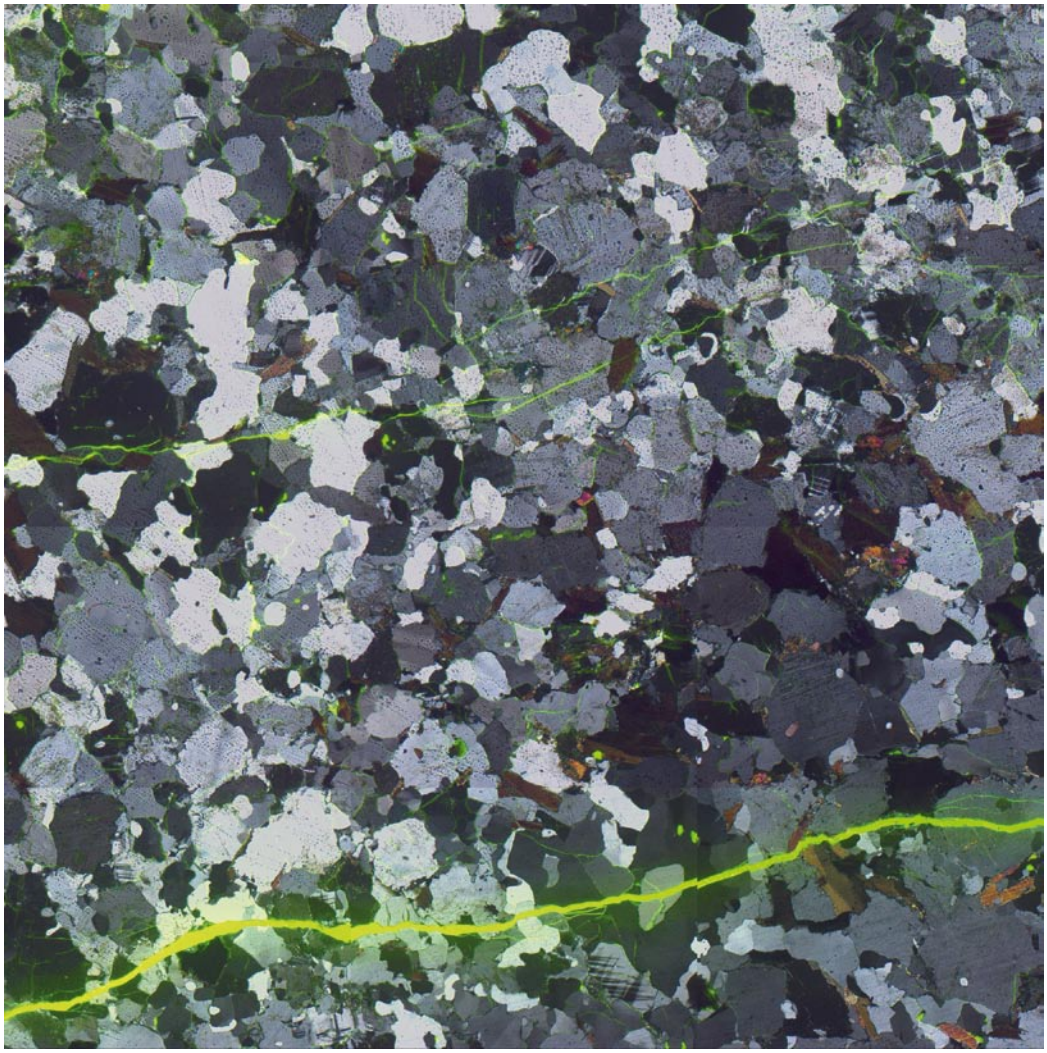

Figure 4-9. *Combined polarised and fluorescent microscopic image of specimen F2B1. Image size is 8.3 x 8.3 mm.*

Table 4-3. Crack density of specimen F2B1, based on linear traverse measurements.

Orientation	Grain boundary (cracks/mm) (%)	Intragranular (cracks/mm) (%)	Transgranular (cracks/mm) (%)	Total (cracks/mm) (%)
Parallel to drill core	1.57/72	0.53/24	0.09/4	2.19
Perpendicular to drill core	2.39/75	0.36/11	0.42/13	2.39
Ratio	0.66	1.47	0.21	0.92

Specimen F2B2

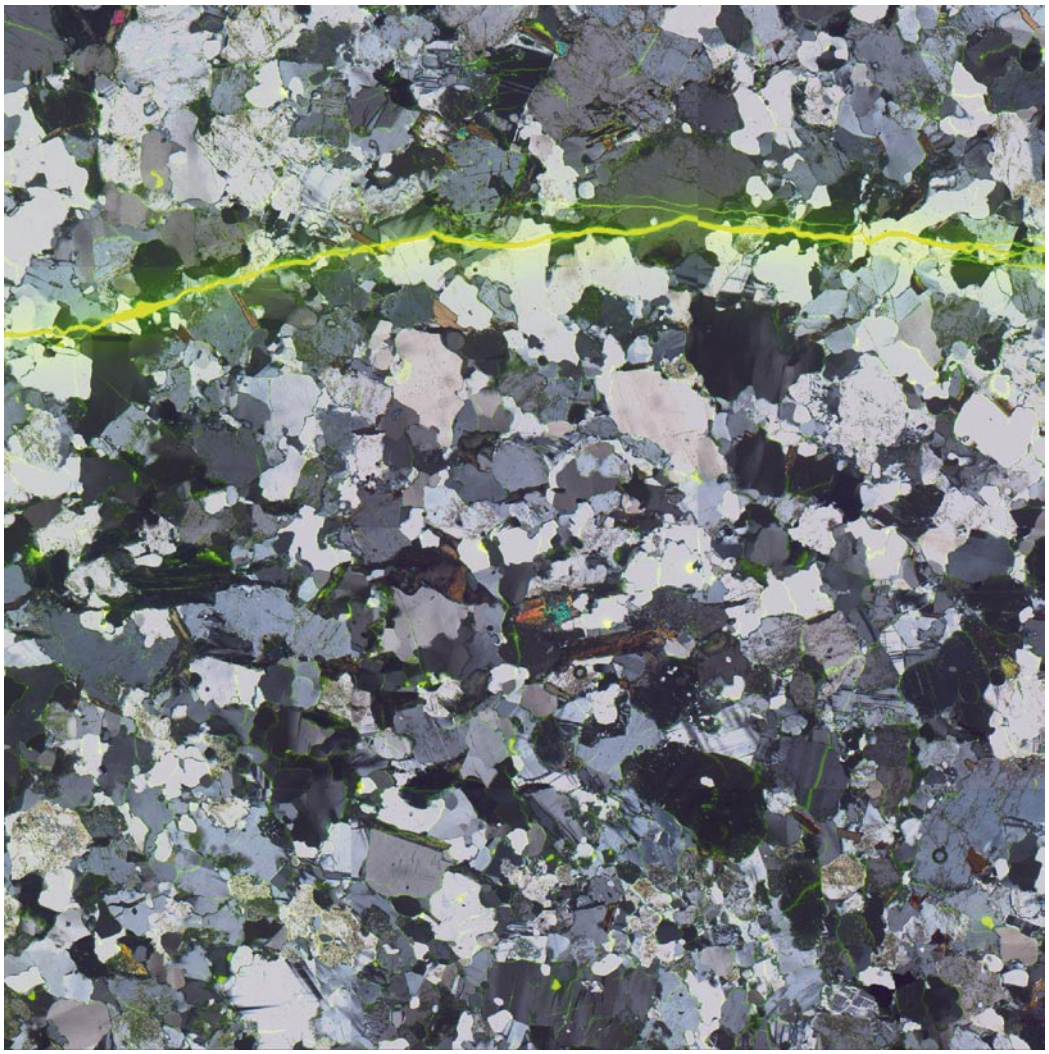

Figure 4-10. *Combined polarised and fluorescent microscopic image of specimen F2B2. Image size is 8.3 x 8.3 mm.*

Table 4-4. Crack density of specimen F2B2, based on linear traverse measurements.

Orientation	Grain boundary (cracks/mm) (%)	Intragranular (cracks/mm) (%)	Transgranular (cracks/mm) (%)	Total (cracks/mm) (%)
Parallel to drill core	2.36/87	0.24/9	0.12/4	2.72
Perpendicular to drill core	2.72/84	0.3/9	0.23/7	3.25
Ratio	0.87	0.8	0.52	0.84

Specimen F4A1

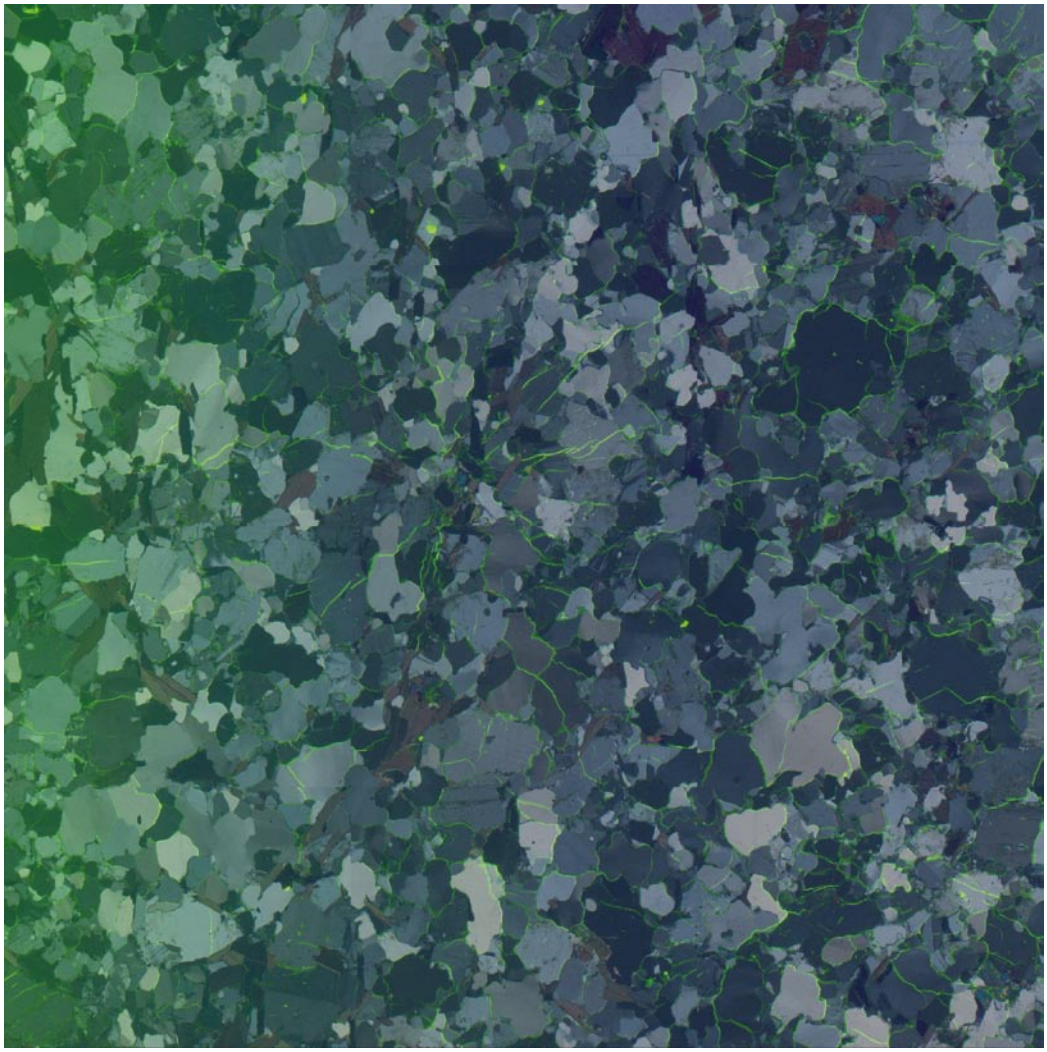

Figure 4-11. *Combined polarised and fluorescent microscopic image of specimen F4A1. Image size is 8.3 x 8.3 mm.*

Table 4-5. Crack density of specimen F4A1, based on linear traverse measurements.

Orientation	Grain boundary (cracks/mm) (%)	Intragranular (cracks/mm) (%)	Transgranular (cracks/mm) (%)	Total (cracks/mm) (%)
Parallel to drill core	2.67/89	0.23/8	0.08/3	2.98
Perpendicular to drill core	2.3/87	0.22/8	0.12/4	2.64
Ratio	1.16	1.05	0.66	1.13

Specimen F4A2

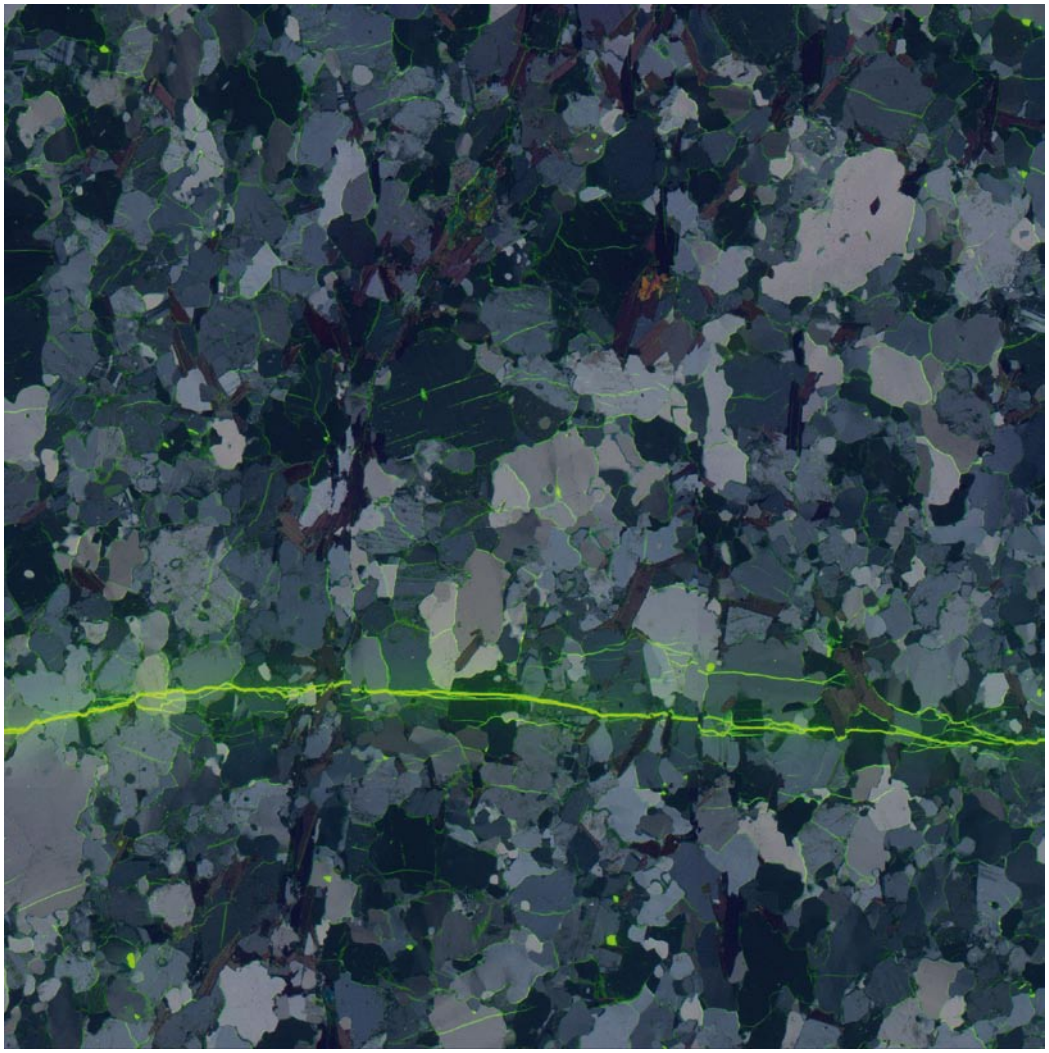

Figure 4-12. *Combined polarised and fluorescent microscopic image of specimen F4A2. Image size is 8.3 x 8.3 mm.*

Table 4-6. Crack density of specimen F4A2, based on linear traverse measurements.

Orientation	Grain boundary (cracks/mm) (%)	Intragranular (cracks/mm) (%)	Transgranular (cracks/mm) (%)	Total (cracks/mm) (%)
Parallel to drill core	1.84/85	0.21/10	0.11/5	2.16
Perpendicular to drill core	1.57/77	0.19/9	0.28/14	1.57
Ratio	1.17	1.11	0.39	1.38

Specimen F4B1

Figure 4-13. *Combined polarised and fluorescent microscopic image of specimen F4B1. Image size is 8.3 x 8.3 mm.*

Table 4-7. Crack density of specimen F4B1, based on linear traverse measurements.

Orientation	Grain boundary (cracks/mm) (%)	Intragranular (cracks/mm) (%)	Transgranular (cracks/mm) (%)	Total (cracks/mm) (%)
Parallel to drill core	2.41/88	0.26/9	0.08/3	2.75
Perpendicular to drill core	2,04/72	0,38/13	0,4/14	2,82
Ratio	1.18	0.68	0.2	0.96

Specimen F2B2

Figure 4-14. *Combined polarised and fluorescent microscopic image of specimen F4B2. Image size is 8.3 x 8.3 mm.*

Table 4-8. Crack density of specimen F4B2, based on linear traverse measurements.

Orientation	Grain boundary (cracks/mm) (%)	Intragranular (cracks/mm) (%)	Transgranular (cracks/mm) (%)	Total (cracks/mm) (%)
Parallel to drill core	2.18/87	0.26/10	0.08/3	2.52
Perpendicular to drill core	1.69/75	0.19/8	0.37/16	2.25
Ratio	1.29	1.37	0.22	1.12

Specimen URL1A

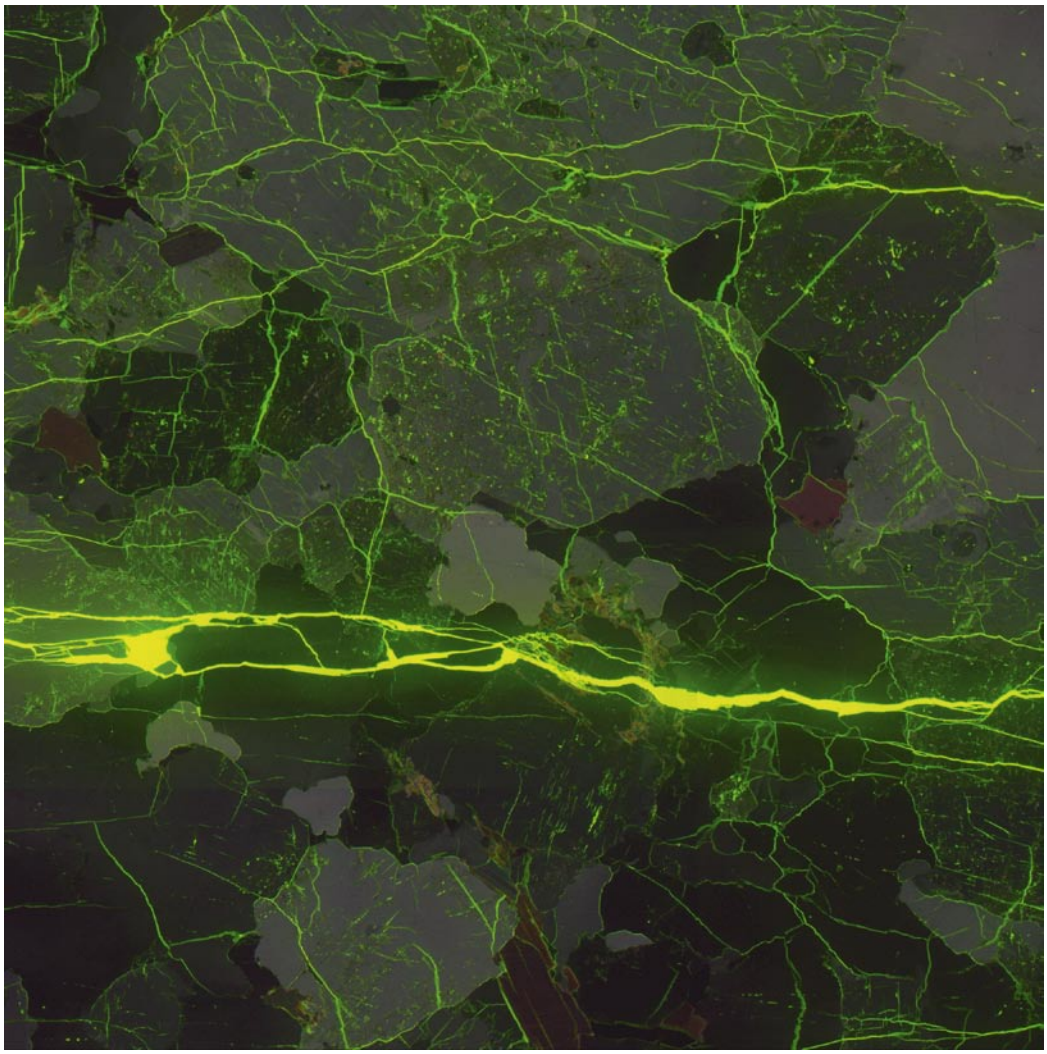

Figure 4-15. *Combined polarised and fluorescent microscopic image of specimen URL1A. Image size is 8.3 x 8.3 mm.*

Table 4-9. Crack density of specimen URL1A, based on linear traverse measurements.

Orientation	**Grainboundary (cracks/mm) (%)**	**Intragranular (cracks/mm) (%)**	**Transgranular (cracks/mm) (%)**	**Total** (cracks/mm) (%)
Parallel to drill core	0.6/39	0.78/51	0.15/10	1.53
Perpendicular to drill core	0.65/31	0.72/35	0.71/34	2.08
Ratio	0.92	1.08	0.25	0.74

Specimen URL1B

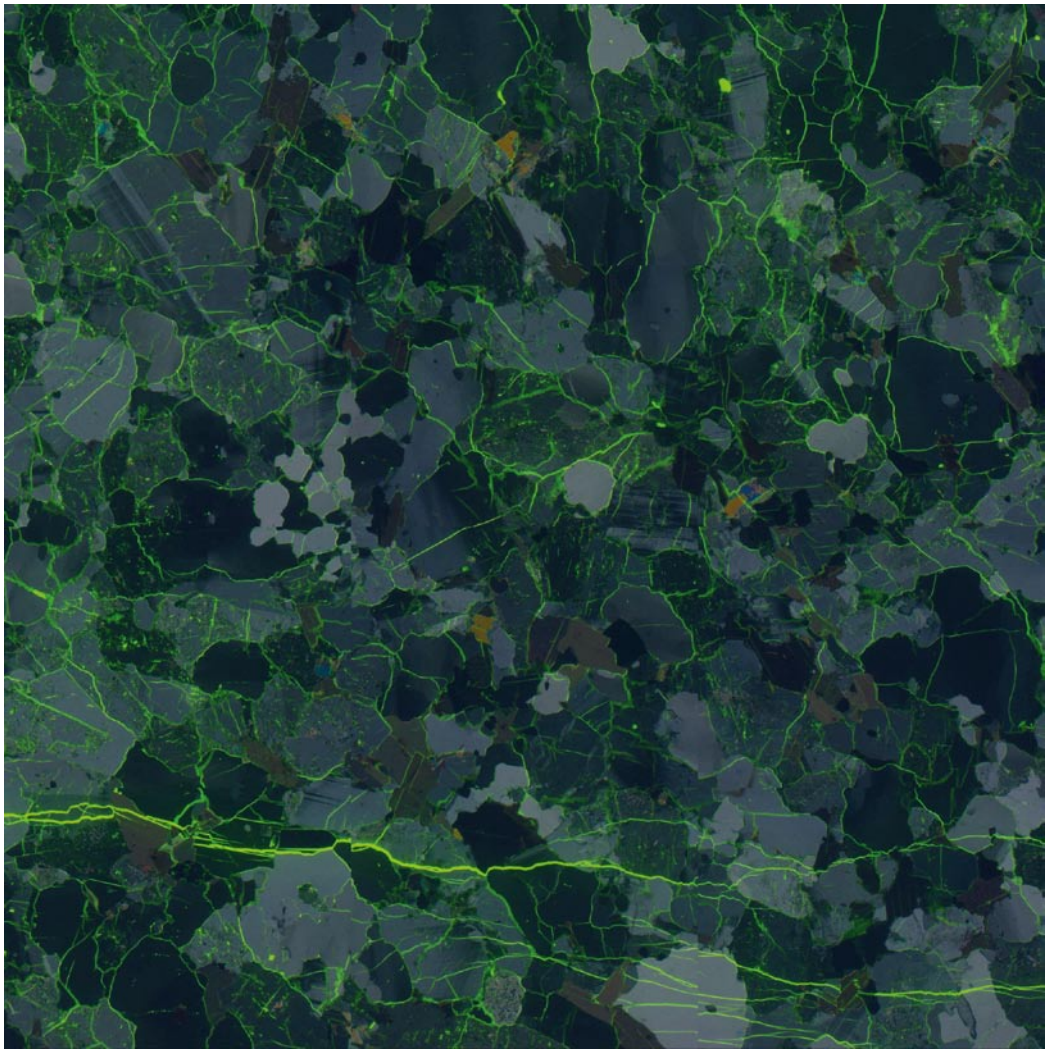

Figure 4-16. *Combined polarised and fluorescent microscopic image of specimen URL1B. Image size is 8.3 x 8.3 mm.*

Table 4-10. Crack density of specimen URL1B, based on linear traverse measurements.

Orientation	Grain boundary (cracks/mm) (%)	Intragranular (cracks/mm) (%)	Transgranular (cracks/mm) (%)	Total (cracks/mm) (%)
Parallel to drill core	1.57/72	0.52/24	0.1/4	2.19
Perpendicular to drill core	1.39/60	0.48/21	0.46/20	2.33
Ratio	1.13	1.08	0.22	0.94

Specimen URL2

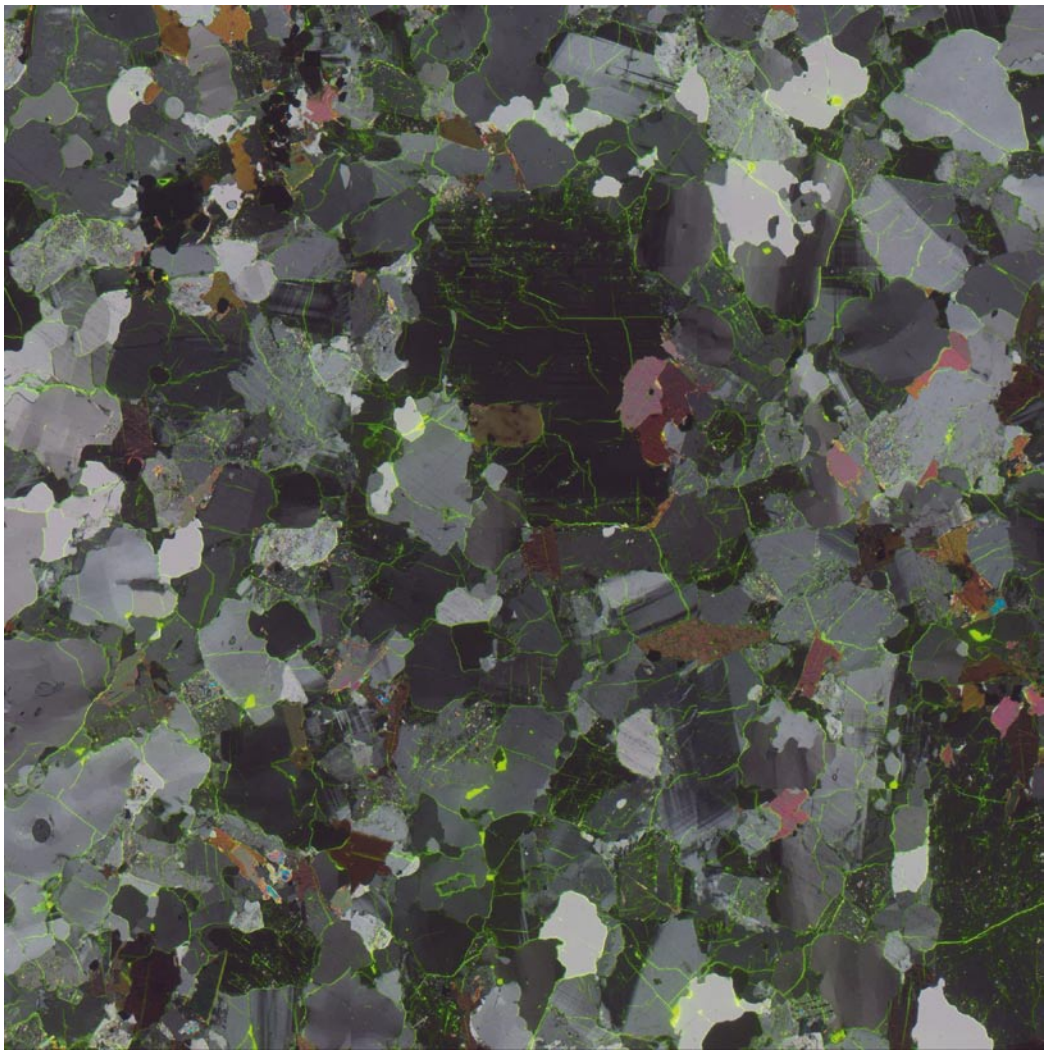

Figure 4-17. *Combined polarised and fluorescent microscopic image of specimen URL2. Image size is 8.3 x 8.3 mm.*

Table 4-11. Crack density of specimen URL2, based on linear traverse measurements.

Orientation	Grainboundary (cracks/mm) (%)	Intragranular (cracks/mm) (%)	Transgranular (cracks/mm) (%)	Total (cracks/mm) (%)
Parallel to drill core	1.48/64	0.71/31	0.12/5	2.31
Perpendicular to drill core	1.27/61	0.64/31	0.18/9	2.09
Ratio	1.17	1.11	0.67	1.11

Specimen URL3

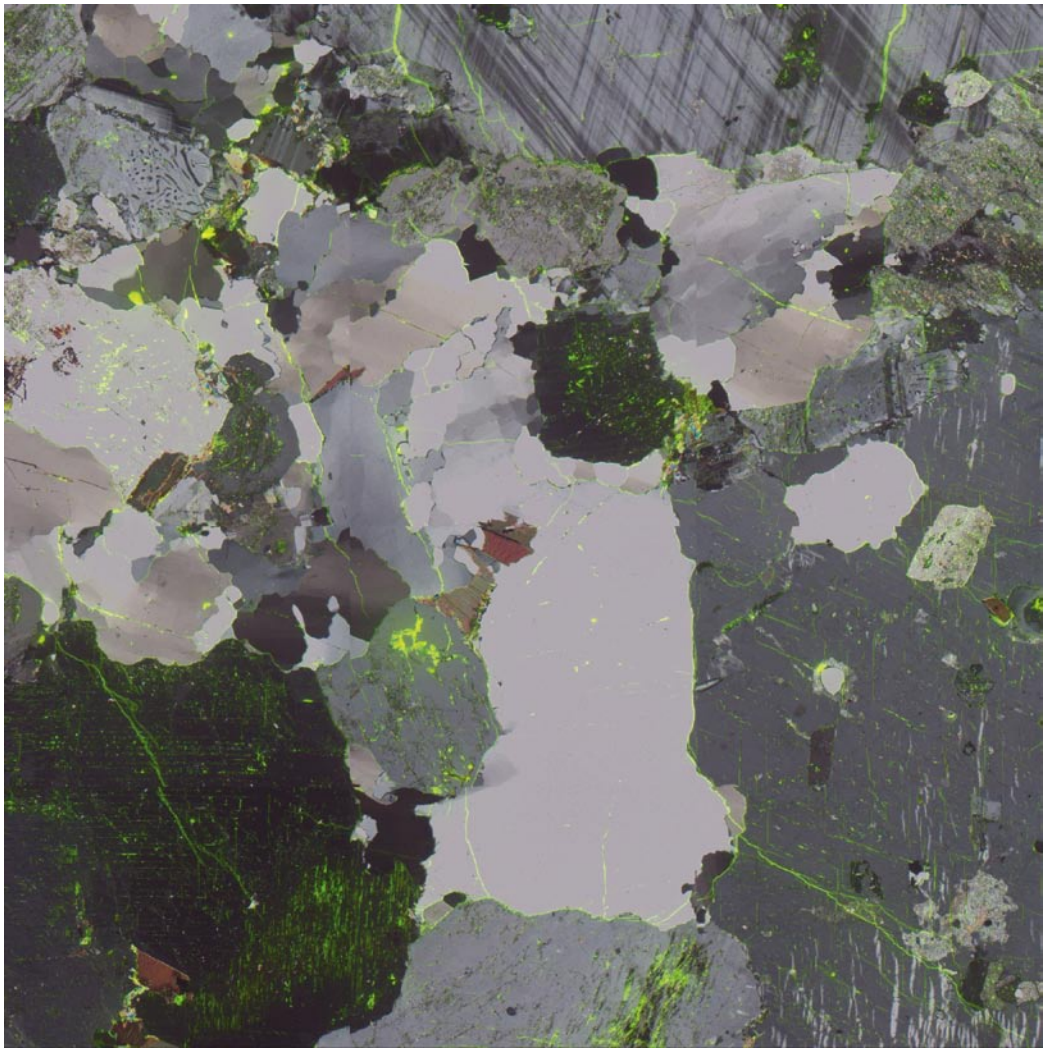

Figure 4-18. *Combined polarised and fluorescent microscopic image of specimen URL3. Image size is 8.3 x 8.3 mm.*

Table 4-12. Crack density of specimen URL3, based on linear traverse measurements.

Orientation	Grain boundary (cracks/mm) (%)	Intragranular (cracks/mm) (%)	Transgranular (cracks/mm) (%)	Total (cracks/mm) (%)
Parallel to drill core	0.53/47	0.49/44	0.1/9	1.12
Perpendicular to drill core	0.51/58	0.28/32	0.09/10	0.88
Ratio	1.04	1.75	1.11	1.27

4.2.2 Part II Length and Orientation of intragranular and transgranular micro cracks

The length and orientation of the intragranular and transgranular micro cracks have been determined using digital image analysis. The length of the micro cracks is defined as the fiber length.

Fiber length = $(P + (P^2–16xA)^{0.5})/4$ where:

P = Perimeter of the object and A is the area of the object.

Specimen F2A1

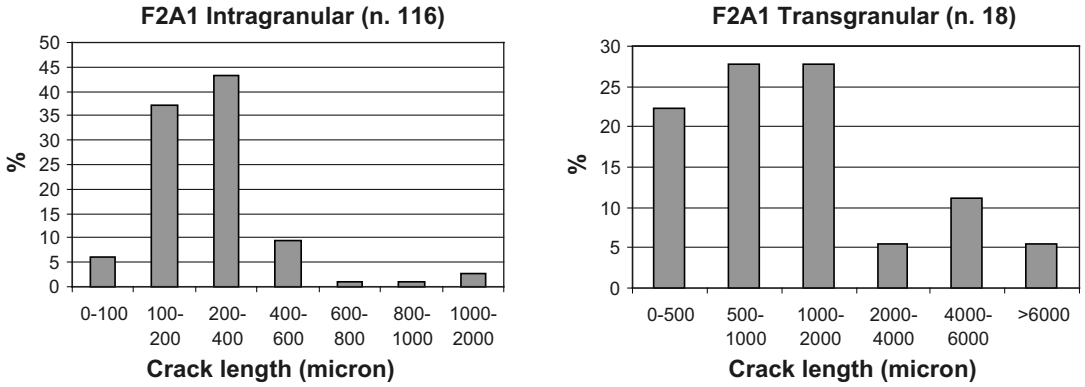

Figure 4-19. *Diagrams showing the size distribution of intragranular and transgranular micro cracks of specimen F2A1.*

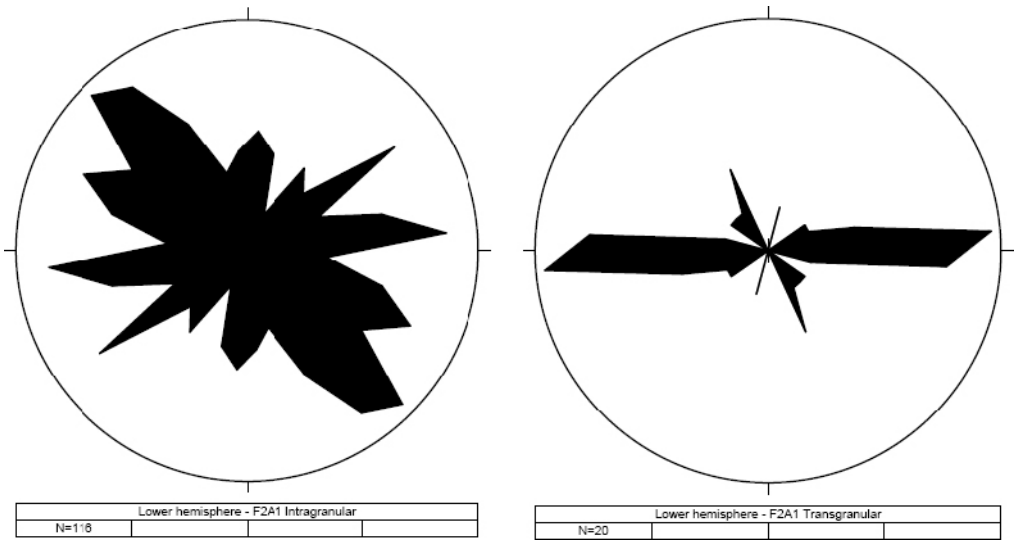

Figure 4-20. *Rose diagrams showing the orientation of intragranular and transgranular micro cracks of specimen F2A1.*

Specimen F2A2

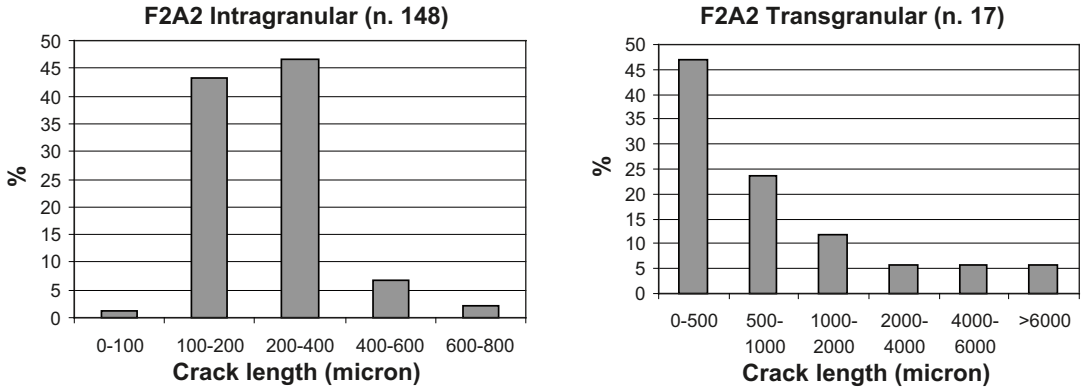

Figure 4-21. *Diagrams showing the size distribution of intragranular and transgranular micro cracks of specimen F2A2.*

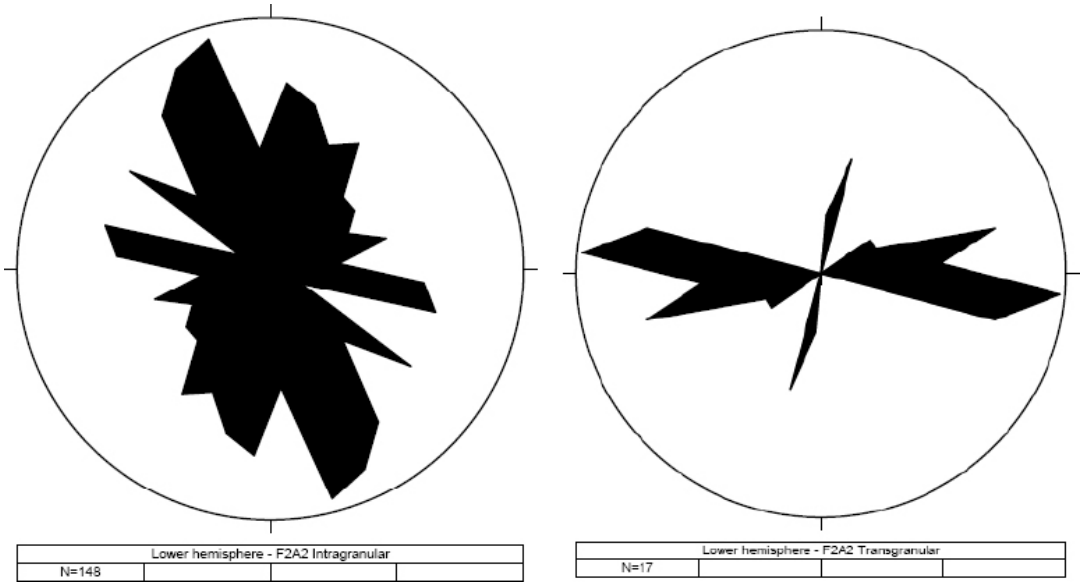

Figure 4-22. *Rose diagrams showing the orientation of intragranular and transgranular micro cracks of specimen F2A1.*

Specimen F2B1

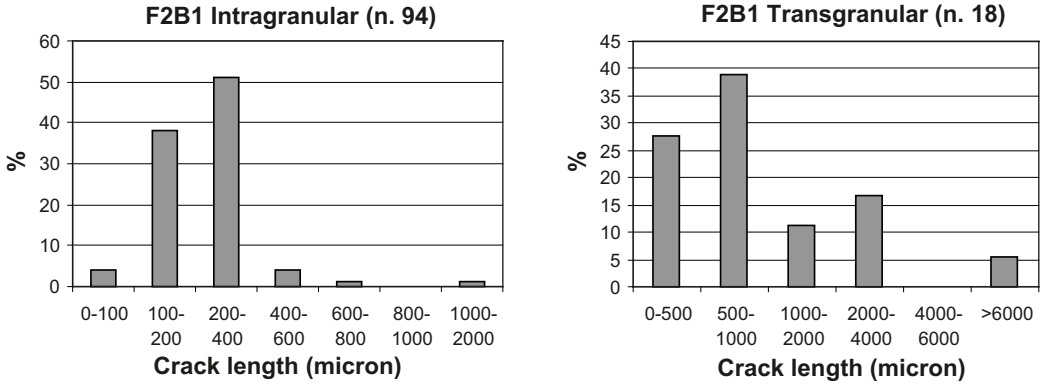

Figure 4-23. *Diagrams showing the size distribution of intragranular and transgranular micro cracks of specimen F2B1.*

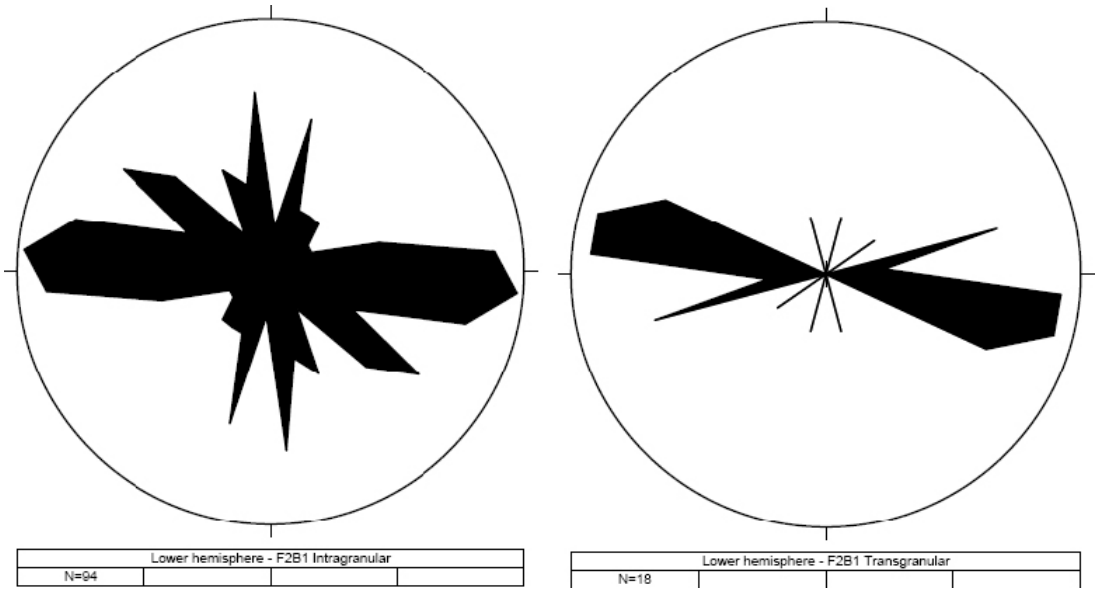

Figure 4-24. *Rose diagrams showing the orientation of intragranular and transgranular micro cracks of specimen F2B1.*

Specimen F2B2

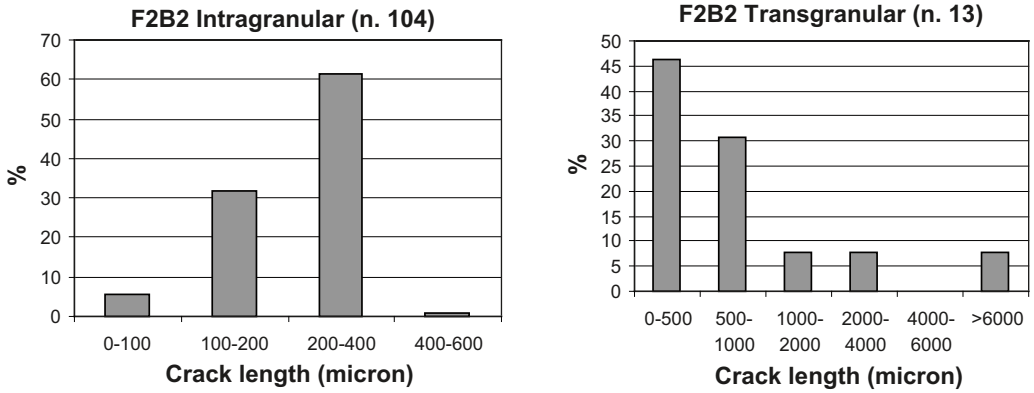

Figure 4-25. *Diagrams showing the size distribution of intragranular and transgranular micro cracks of specimen F2B2.*

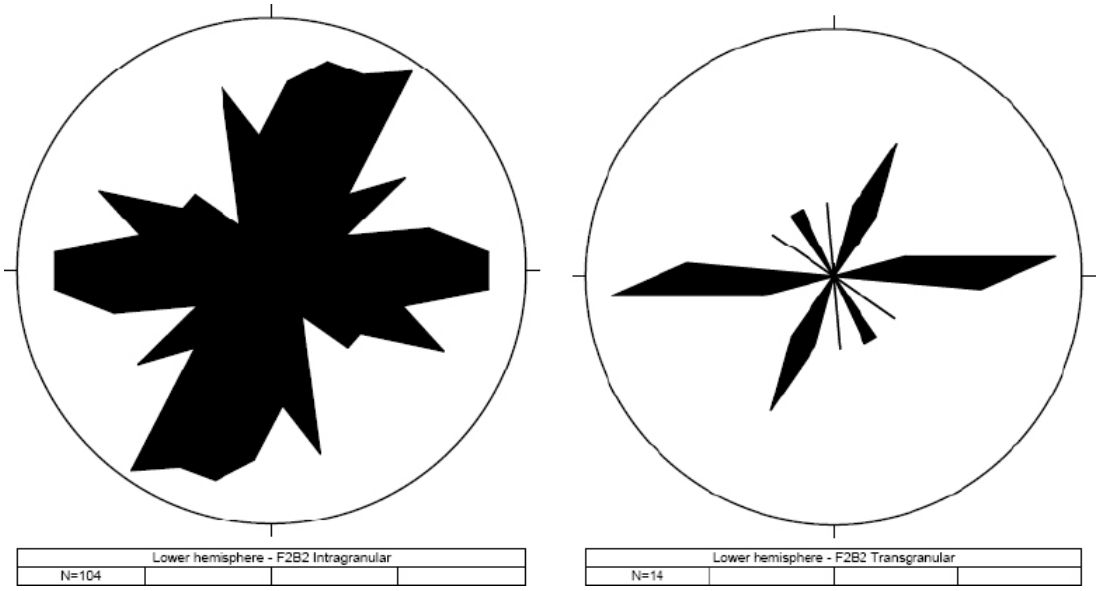

Figure 4-26. *Rose diagrams showing the orientation of intragranular and transgranular micro cracks of specimen F2B2.*

Specimen F4A1

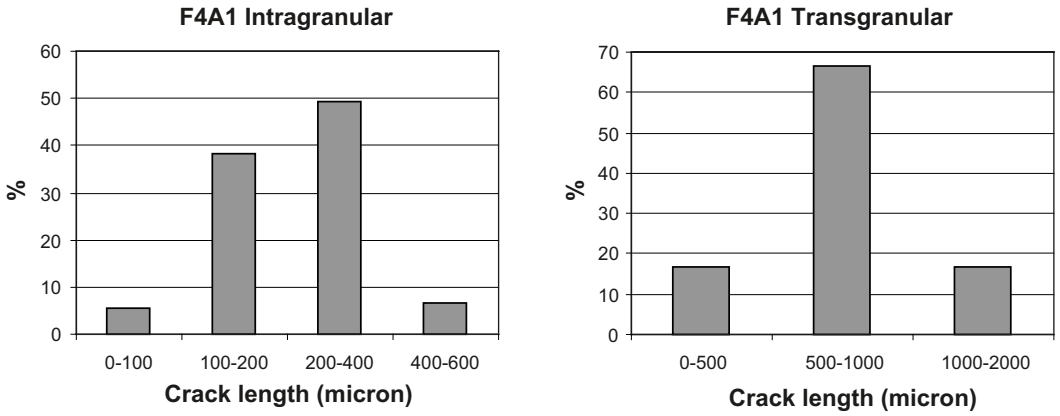

Figure 4-27. *Diagrams showing the size distribution of intragranular and transgranular micro cracks of specimen F4A1.*

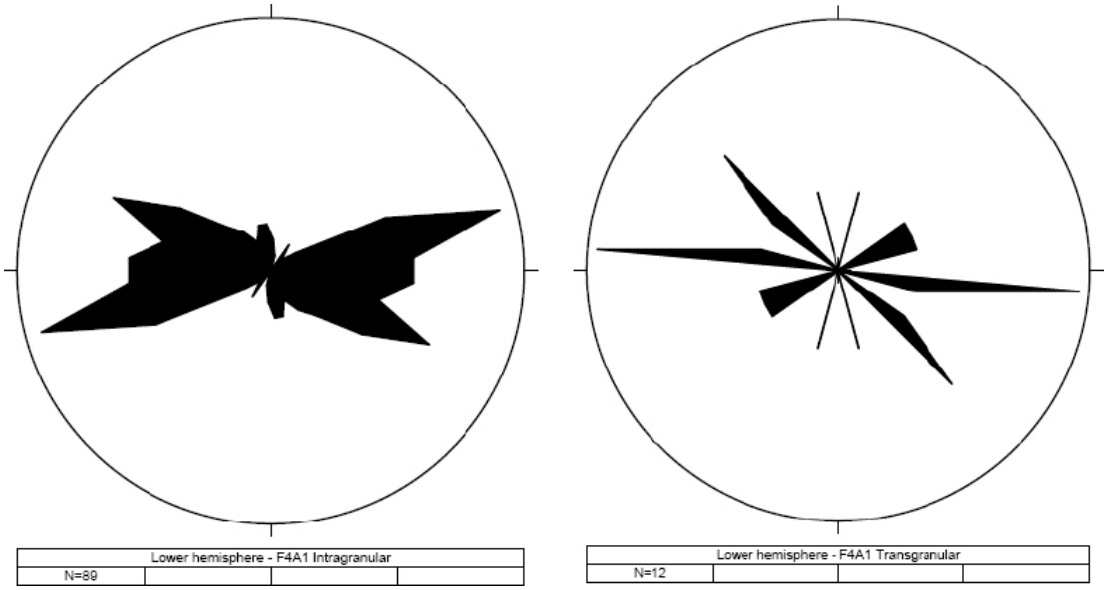

Figure 4-28. *Rose diagrams showing the orientation of intragranular and transgranular micro cracks of specimen F4A1.*

Specimen F4A2

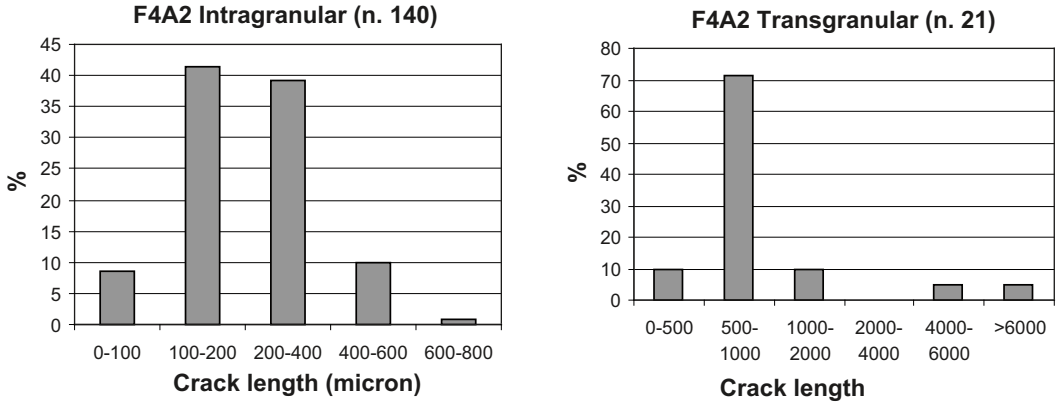

Figure 4-29. *Diagrams showing the size distribution of intragranular and transgranular micro cracks of specimen F4A2.*

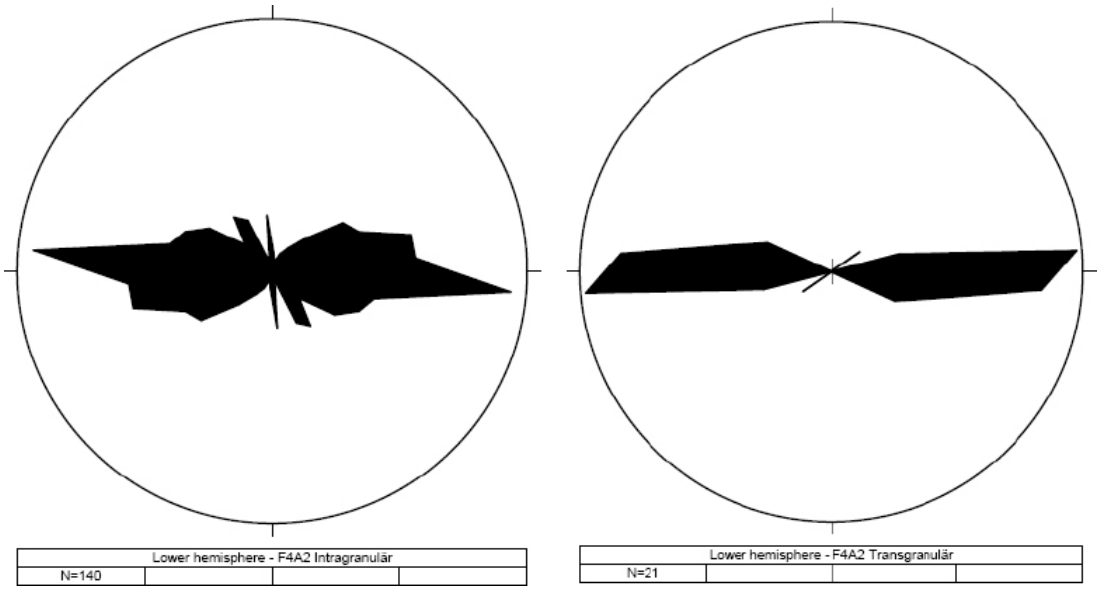

Figure 4-30. *Rose diagrams showing the orientation of intragranular and transgranular micro cracks of specimen F4A2.*

Specimen F4B1

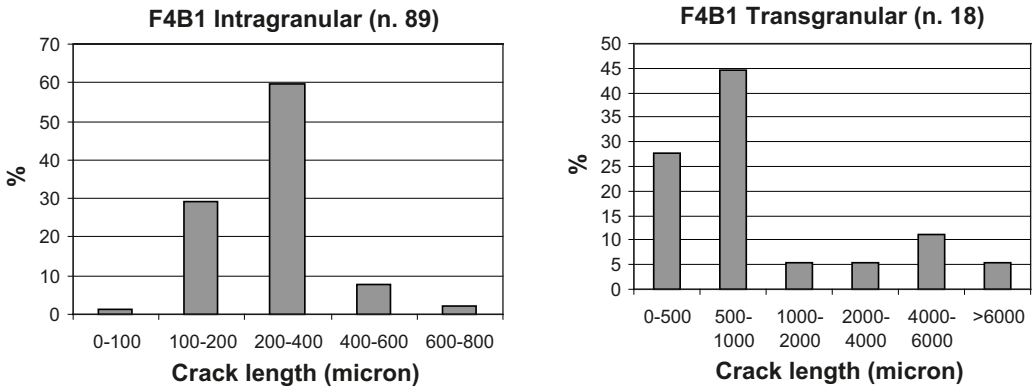

Figure 4-31. *Diagrams showing the size distribution of intragranular and transgranular micro cracks of specimen F4B1.*

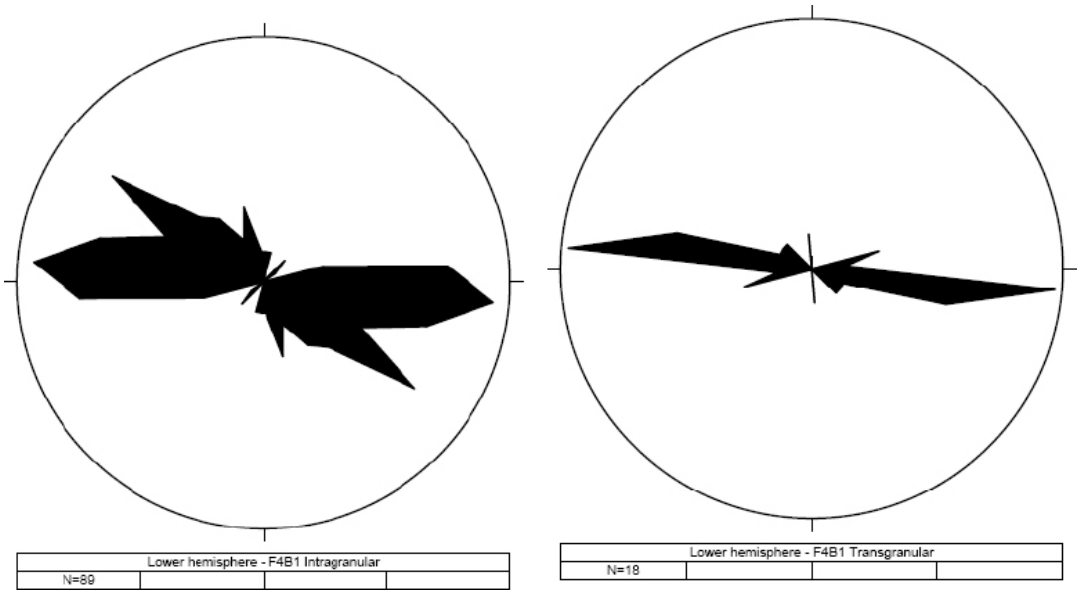

Figure 4-32. *Rose diagrams showing the orientation of intragranular and transgranular micro cracks of specimen F4B1.*

Specimen F4B2

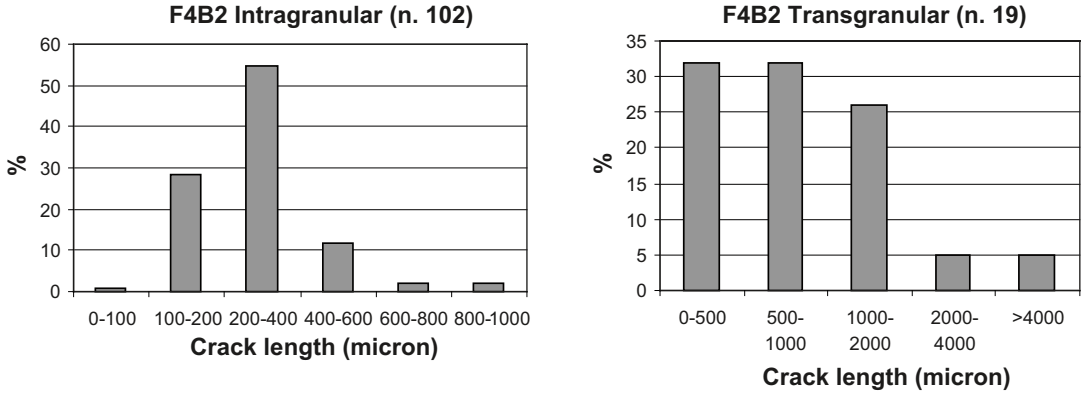

Figure 4-33. *Diagrams showing the size distribution of intragranular and transgranular micro cracks of specimen F4B2.*

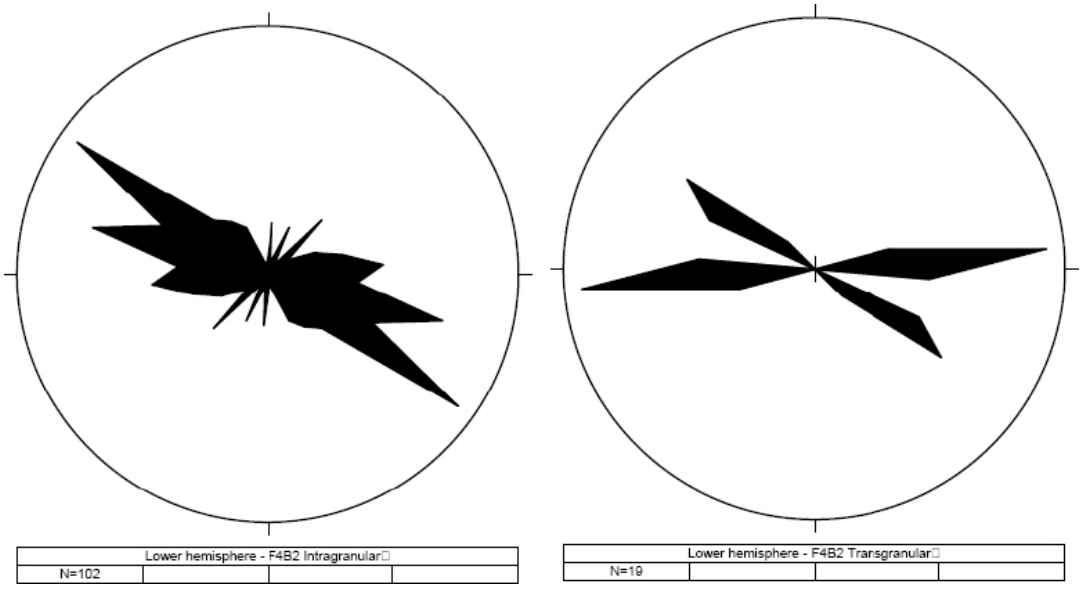

Figure 4-34. *Rose diagrams showing the orientation of intragranular and transgranular micro cracks of specimen F4B2.*

Specimen URL1A

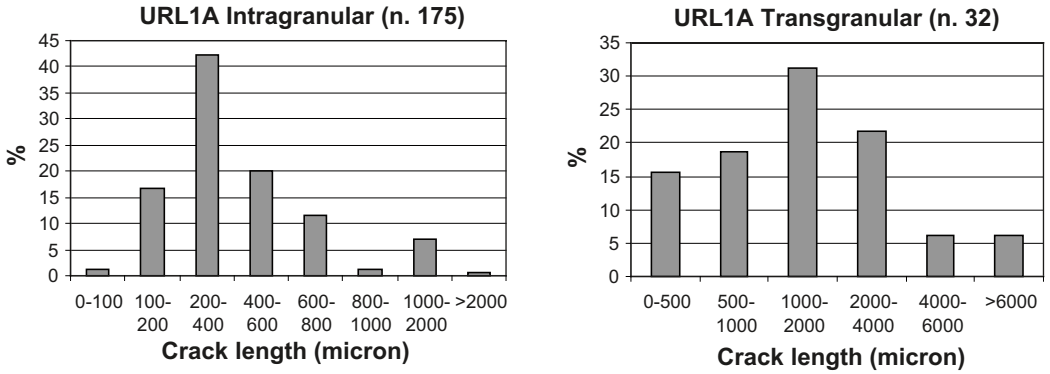

Figure 4-35. *Diagrams showing the size distribution of intragranular and transgranular micro cracks of specimen URL1A.*

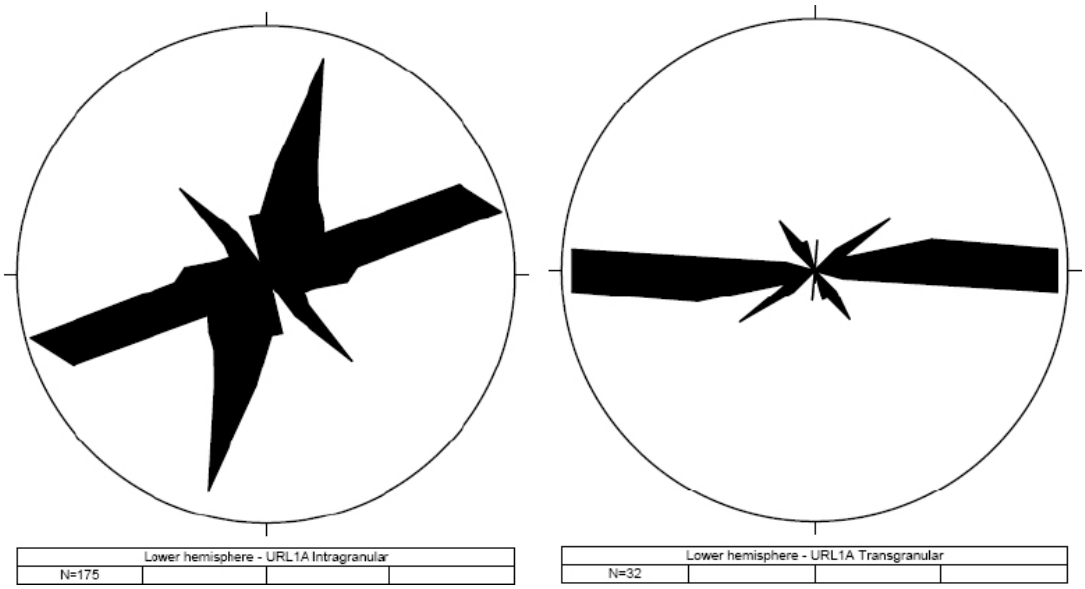

Figure 4-36. *Rose diagrams showing the orientation of intragranular and transgranular micro cracks of specimen URL1A.*

Specimen URL1B

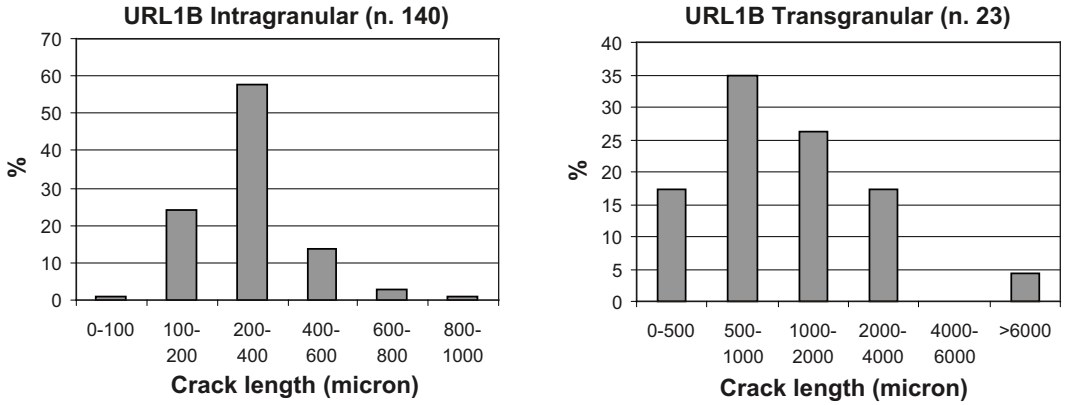

Figure 4-37. *Diagrams showing the size distribution of intragranular and transgranular micro cracks of specimen URL1B.*

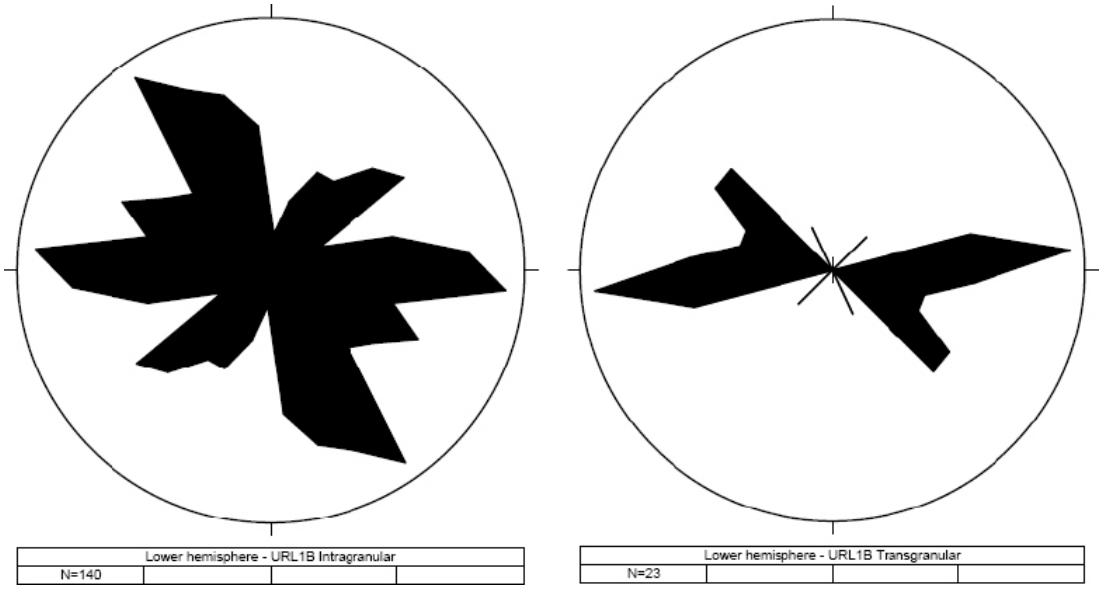

Figure 4-38. *Rose diagrams showing the orientation of intragranular and transgranular micro cracks of specimen URL1B.*

Specimen URL2

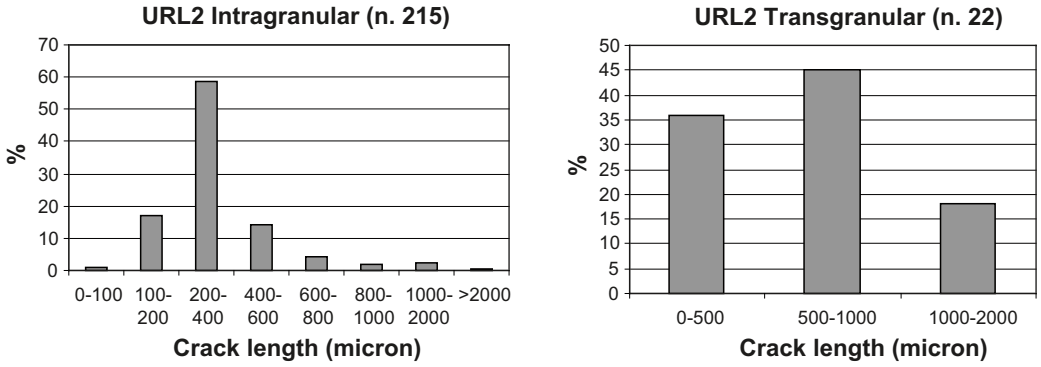

Figure 4-39. *Diagrams showing the size distribution of intragranular and transgranular micro cracks of specimen URL2.*

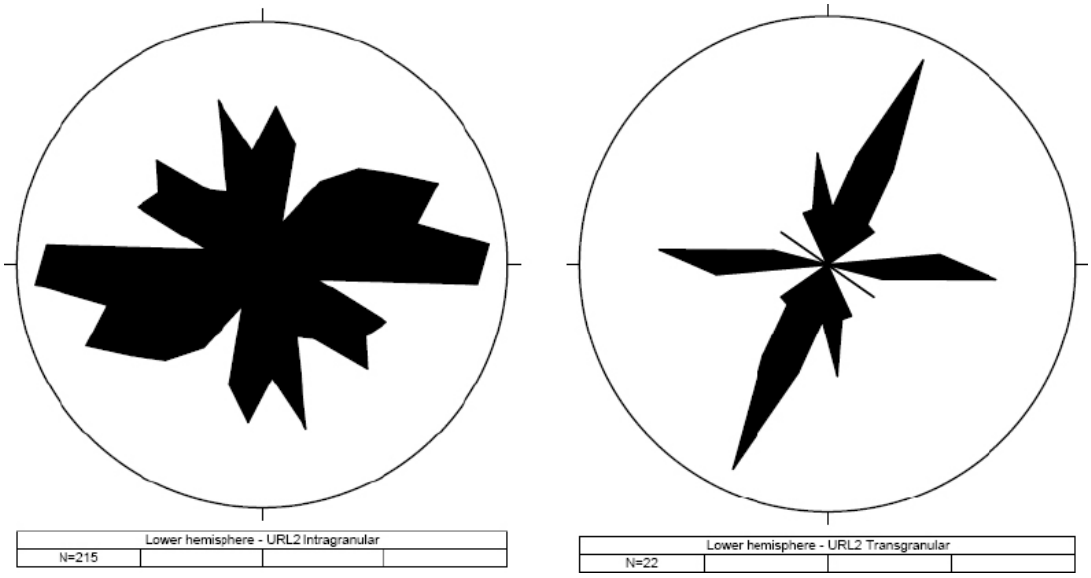

Figure 4-40. *Rose diagrams showing the orientation of intragranular and transgranular micro cracks of specimen URL2.*

Specimen URL3

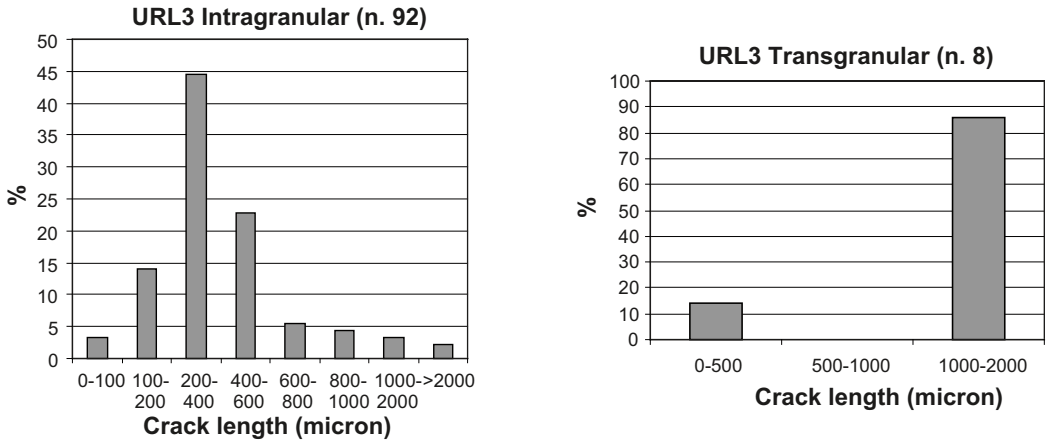

Figure 4-41. *Diagrams showing the size distribution of intragranular and transgranular micro cracks of specimen URL3.*

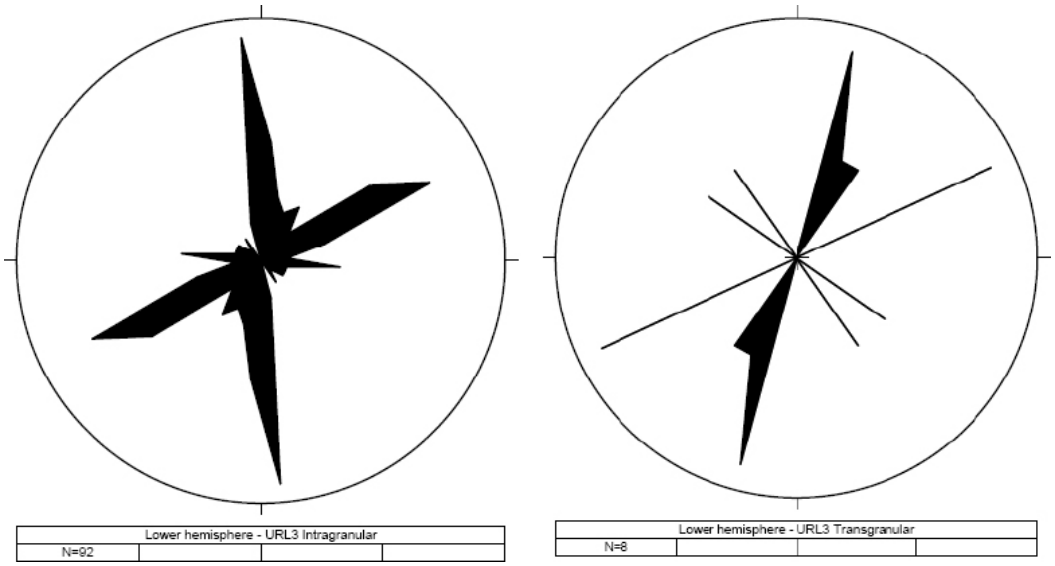

Figure 4-42. *Rose diagrams showing the orientation of intragranular and transgranular micro cracks of specimen URL3.*

5 Discussion

The results showed that mainly transgranular micro cracks were formed due to the core disking, and these cracks are mainly situated within 1 mm from the large cracks that form the typical crack pattern for the core disking phenomena (e.g. Figure 3-2).

According to the results is the rock between the large transgranular cracks rather undisturbed. This feature is shown for all specimens.

The transgranular cracks easily propagate through quartz and feldspar minerals, but when they meet a biotite the crack propagation stops or continues around the biotite (Figure 5-1). There are very few transgranular cracks that not hit the mantle of the core which indicates that the transgranular cracks starts from the mantle of the core and propagate through the whole core or stop in the centre of the core.

The linear traverse measurements show a small trend that there are more grain boundary and intragranular micro cracks that are oriented parallel to the drill core, especially for the Forsmark specimens. One suggestion for this result could be that existing micro cracks close when the core disking occurs.

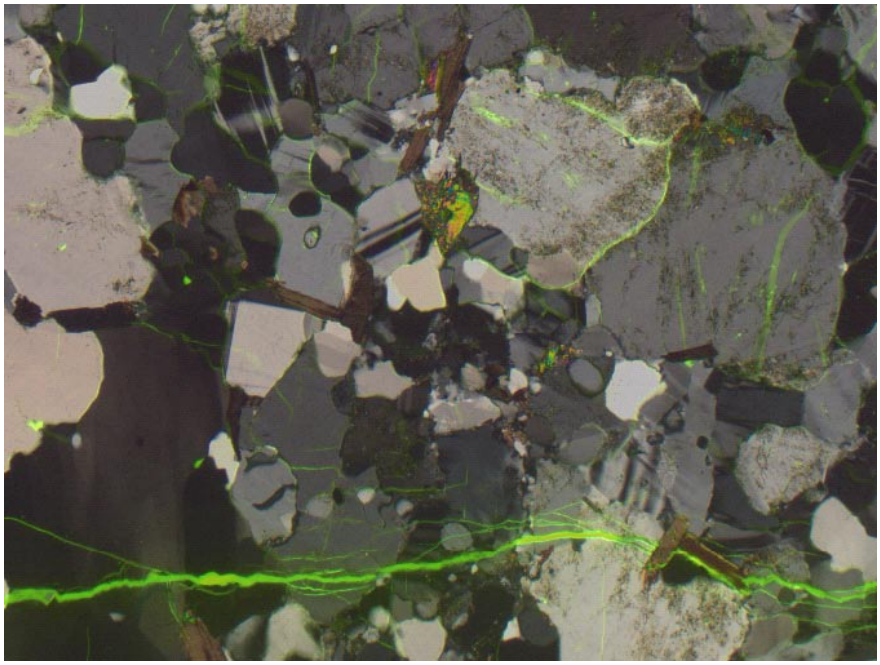

Figure 5-1. *Combined polarised and fluorescent microscopic image of specimen F2A2, showing how the cracks propagate around the biotite. Image size is 2.8 x 2.1 mm.*